Construction of a high-density high-resolution genetic map and its integration with BAC-based physical map in channel catfish

by

Yun Li

A dissertation submitted to the Graduate Faculty of
Auburn University
in partial fulfillment of the
requirements for the Degree of
Doctor of Philosophy

Auburn, Alabama
December 12, 2015

Keywords: SNP, catfish, linkage map,
physical map, genome

Approved by

Zhanjiang Liu, Chair, Professor of School of Fisheries, Aquaculture, and Aquatic Sciences
Rex Dunham, Professor of School of Fisheries, Aquaculture, and Aquatic Sciences
Nannan Liu, Professor of Insect Molecular Toxicology and Physiology
Charles Y. Chen, Associate Professor of Crop, Soil and Environmental Sciences

Abstract

Catfish is the leading aquaculture specie in the United States of American. However, the catfish industry is facing great challenges due to devastating diseases, high production cost, high feed and energy cost and international competition. Exploiting fish genetics and genomics can greatly contribute to production efficiency and enhancing performance. Construction of genetic linkage map is essential for genetic and genomic studies. Recent advances in sequencing and genotyping technologies made it possible to generate high-density and high-resolution genetic linkage maps, especially for the organisms lacking extensive genomic resources. In the present work, we constructed a high-density and high-resolution genetic map for channel catfish with three large resource families genotyped using the catfish 250K SNP array. A total of 54,342 SNPs were placed on the linkage map, the highest marker density among all aquaculture species. The estimated genetic size was 3,505 cM with a resolution of 0.22 cM for sex-averaged genetic map. The sex-specific linkage maps spanned a total of 4,495 cM in females and 2,594 cM in males, representing a ratio of 1.7:1 between female and male in recombination rate. After integration with previously established physical map, over 87% of physical map contigs were anchored to the linkage groups which covered a physical length of 867 Mb, accounting for about 90% of the catfish genome. The integrated map provides a valuable tool for validating and improving the catfish whole genome assembly, and facilitates fine-scale QTL mapping and positional cloning of genes responsible for economically important traits.

Acknowledgments

I would like to express my deep and sincere gratitude to my supervisor, Dr. Zhanjiang Liu, for his expertise, guidance, understanding and support during my Ph.D. study. I would also like to thank my committee members: Dr. Rex Dunham, Dr. Nannan Liu, and Dr. Charles Y. Chen, and to thank my outside reader Dr. Luxin Wang for their insightful comments and assistance of my degree program. I am grateful to Dr. Shikai Liu, whose guidance, encouragement, and kindness help me from various perspectives. I am very grateful for the technical assistance by Dr, Huseyin Kucuktas and Ludmilla Kaltenboeck. My thanks also goes to Dr. Ruijia Wang, Dr. Luyang Sun, Dr. Jiaren Zhang, Dr. Lin Song, Jun Yao, Chen Jiang, Lisui Bao, Xin Geng, Ailu Chen, Xiaozhu Wang, Qifan Zeng, Sen Gao, Tao Zhou, Ning Li, Qiang Fu and all the other colleagues in the laboratory for their help, collaboration and friendship. I am grateful to the Chinese Scholarship Council for the financial support.

Finally, I would like to thank my family: my father Xin Li, my mother Jingzhao Hu and my fiancé Zhenkui Qin for their constant love and support.

Table of Contents

List of Tables

List of Figures

CHAPTER I

INTRODUCTION

Channel catfish, *Ictalurus punctatus*, is a member of order Siluriformes, and it belongs to the bullhead catfish family, Ictaluridae, and is the primary aquaculture species in the United States. However, as culture of catfish intensifies, outbreaks of diseases are becoming increasingly common and cause an annual loss of almost 100 million dollars. In addition, the industry is currently struggling to unprecedented challenges due to the increasing feed and energy cost, production inefficiencies and international competition (Hanson and Sites, 2012). The future of catfish industry, the leading aquaculture industry in the US, is threatened if the production and production efficiency are not improved. Although incremental improvements can be made in various aspects of aquaculture practices such as use of more efficient culture systems. E.e., in pond raceways, improvements in feed, reduction in energy cost and various other measures, exploiting genetics can greatly contribute to increasing production efficiency and improving performance traits.

For the purpose of genetic improvement, genetic linkage maps are essential for the understanding of genomic levels of organization of inheritance of traits (Myers et al., 2005), for comparative genome analysis (Liu et al., 2009), and fine-scale QTL mapping and positional cloning of genes responsible for performance and production traits (Palti et al., 2012). In addition, genetic linkage maps are valuable resources for the generation of chromosome-level assembly of

whole-genome sequences and for comparative genome analysis (Kucuktas et al., 2009). In most of the recent whole genome sequencing cases, whole genome sequences are generated using next generation sequencing. Short sequencing reads are assembled into contigs. Such contigs are generally still relatively short in size although they vary in sizes from several kilobases to tens of kilobases. Increases in genome sequencing coverage and sequencing libraries can increase the quality of the assembly allowing the sizes of contigs to be increased. However, next generation sequencing methods alone cannot provide the resources to assemble complex genomes at the chromosomal level. Genome sequence assemblies at the chromosomal level require the assembly of tens of thousands to hundreds of thousands of contigs.

Highly segmented genome assemblies prohibit efficient genome analysis. Therefore, various genome resources have been created to reduce the segmentation of the genome assemblies. One of these resources is physical maps constructed by analysis of the large-insert genomic libraries. Historically, several types of large insert libraries have been used. These include yeast artificial chromosomes (YACs, Burke et al., 1987), bacterial artificial chromosomes (BACs, McPherson et al., 2001) and Cosmid-based libraries (Eiglmeier et al., 1993). YACs have the largest capacity for cloning very large inserts, but they are relatively instable leading to inter-clone recombinations, and therefore their use in genome studies has been limited. Cosmid libraries have the smallest capacity for cloning the large inserts, most often limited to approximately 40 Kb, and therefore, their use in large insert libraries has also been limited. BACs are the most popular large insert libraries as they are stable, and can hold inserts of up to 200 kb. BAC-based physical maps can organize the entire genome into restriction fingerprints-based contigs. Such contigs are similar to the whole genome sequencing contigs, but are constructed using overlapping restriction enzyme fingerprints rather than overlapping sequences themselves for the whole genome sequence

assemblies. By analysis of restriction fingerprints of overlapping genomic clones of BAC inserts, the whole genome can be organized into a limited number of contigs, most often in the thousands. For instance, the catfish physical maps had 3,307 contigs (Xu et al., 2007) and 1,891 contigs (Quiniou et al., 2007). The integrated catfish physical map included over 2500 contigs (unpublished).

Integration of physical maps and whole genome sequence contigs allows the relationship to be established between the sequence-based contigs and the restriction fingerprints-based contigs, thereby reducing the levels of segmentation of the genome. One of the major applications of genetic linkage map is to integrate physical maps and whole genome assemblies. Integration of genetic map with physical map is useful for understanding genomes from different dimensions, and is essential for comparative genome analysis (Liu et al., 2009), fine-scale QTL mapping and positional cloning of genes responsible for performance and production traits (Ninwichian et al., 2012; Palti et al., 2012). In aquaculture fish species, genetic maps have been constructed in a few species, such as Asian seabass (Wang et al., 2011), Atlantic salmon (Lien et al., 2011), half-smooth tongue sole (Song et al., 2012), rainbow trout (Rexroad et al., 2008), common carp (Zhao et al., 2013) and catfish (Kucuktas et al., 2009; Liu et al., 2003; Ninwichian et al., 2012; Waldbieser et al., 2001). These maps harbor several hundreds to a couple of thousands of markers. The marker densities with these maps are relatively low, with which QTL for agriculturally important performance and production traits can only be mapped in large genomic intervals.

Integrated maps have been developed in several aquaculture fish species using low-density genetic maps. In Atlantic salmon, bacterial artificial chromosome (BAC)-anchored SNP markers were developed to enable the integration of physical and genetic maps by assigning 73 BAC contigs to Atlantic salmon linkage groups (Lorenz et al., 2010). The second generation of rainbow

trout integrated map anchored up to 265 contigs to the genetic map, covering approximately 11% of the genome (Palti et al., 2012). In common carp, a total of 463 physical map contigs and 88 single BACs were integrated into the genetic linkage map, which covered 30% of the common carp genome (Zhao et al., 2013). In catfish, 2,030 BAC end sequence (BES)-derived microsatellites from 1,481 physical map contigs were used for linkage map construction, which anchored 44.8% of the catfish BAC physical map contigs, covering approximately 52.8% of the genome (Ninwichian et al., 2012). Apparently, the level of integration is dependent on the density and resolution of the genetic maps.

The first objective of my study was to construct a high-density and high-resolution genetic linkage map by using a large number of molecular markers covering the entire genome and a large resource panel for linkage mapping analysis. In addition to this primary goal, the second goal was to increase integration of the linkage and physical maps using markers derived from BAC end sequences for genetic linkage analysis.

Our previous genetic linkage analysis used mostly microsatellite markers. In spite of their high polymorphism, and low cost of single marker genotyping, an analysis of tens of thousands of microsatellites with a large number of mapping fish is extremely laborious and cost-prohibitive. Single nucleotide polymorphisms (SNPs) overcome these difficulties by providing high efficiency and low cost large-scale genotyping. SNPs have become markers of choice because of their abundance, even genomic distribution, and easy adaptation to automation (Baird et al., 2008). Recent advances in next generation sequencing (NGS) have allowed rapid discovery of genome-wide SNPs in any organism in a cost-effective manner (Davey et al., 2011). With the availability of large numbers of SNPs, high-density SNP array platform can be developed for high-throughput and efficient genotyping. Alternatively, NGS-based genotyping by sequencing (GBS) (Baird et al.,

2008; Davey et al., 2011; Miller et al., 2007) is also highly efficient. SNP arrays and GBS have both been used to genotype large-scale SNPs for genetic mapping and association analyses (Anderson et al., 2012; Everett et al., 2012; Gonen et al., 2014; Gutierrez et al., 2012; Houston et al., 2014; Lien et al., 2011; McCue et al., 2012; Palaiokostas et al., 2013). Compared to GBS, SNP arrays are more cost-effective. In addition, they provide a greater level of genome coverage. For instance, in most cases, the total number of commonly analyzed SNPs is limited to several thousand while millions of SNPs can be analyzed by using very high density SNP arrays. In addition, GBS of large resource panels for high resolution maps are cost-prohibitive.

Channel catfish is the primary aquaculture species in the United States. Since the initiation of genome research over two decades ago, several genetic maps have been constructed with different types of molecular markers and various resource families (Kucuktas et al., 2009; Liu et al., 2003; Ninwichian et al., 2012; Waldbieser et al., 2001). Up to date, the highest density map was developed to contain 2,030 microsatellites and 100 SNPs (Ninwichian et al., 2012). Although this genetic map has been very useful for genetic and genomic analysis (Jiang et al., 2013; Zhang et al., 2013), marker density in this map was still fairly low and only facilitated integration to the physical map for approximately 52% of catfish genome. Recently, following efforts on expand catfish genomic resources, we have identified millions of SNPs in channel catfish (Liu et al., 2011; Sun et al., 2014) and developed high-density SNP arrays (Liu et al., 2014), which provided the opportunity to develop a high-density and high-resolution SNP-based genetic map. Here we report the construction of genetic linkage map with over 54,000 SNPs in channel catfish, which is, to the best of our knowledge, the highest density genetic map for any aquaculture species. Along with the high density of markers, the utilization of BAC-associated SNPs also allowed significant increase of the integration of the genetic linkage map with the BAC-based physical map in catfish,

allowing over 90% of the catfish genome physical map contigs to be mapped to linkage groups. This genetic map should serve as a valuable framework for validating the reference whole-genome sequences, extensive comparative and functional genomic studies, and fine-scale QTL mapping and association studies in catfish.

References

Anderson, J.L., Mari, A.R., Braasch, I., Amores, A., Hohenlohe, P., Batzel, P., Postlethwait, J.H., 2012. Multiple Sex-Associated Regions and a Putative Sex Chromosome in Zebrafish Revealed by RAD Mapping and Population Genomics. PloS one 7: e40701.

Baird, N.A., Etter, P.D., Atwood, T.S., Currey, M.C., Shiver, A.L., Lewis, Z.A., Selker, E.U., Cresko, W.A., Johnson, E.A., 2008. Rapid SNP discovery and genetic mapping using sequenced RAD markers. PloS one 3, e3376.

Burke, D.T., Carle, G.F., Olson, M.V., 1987. Cloning of large segments of exogenous DNA into yeast by means of artificial chromosome vectors. Science 236, 806-812.

Davey, J.W., Hohenlohe, P.A., Etter, P.D., Boone, J.Q., Catchen, J.M., Blaxter, M.L., 2011. Genome-wide genetic marker discovery and genotyping using next-generation sequencing. Nature reviews. Genetics 12, 499-510.

Eiglmeier, K., Honore, N., Woods, S., Caudron, B., Cole, S., 1993. Use of an ordered cosmid library to deduce the genomic organization of *Mycobacterium leprae*. Molecular microbiology 7, 197-206.

Everett, M.V., Miller, M.R., Seeb, J.E., 2012. Meiotic maps of sockeye salmon derived from massively parallel DNA sequencing. BMC genomics 13, 521.

Gonen, S., Lowe, N.R., Cezard, T., Gharbi, K., Bishop, S.C., Houston, R.D., 2014. Linkage maps of the Atlantic salmon (*Salmo salar*) genome derived from RAD sequencing. BMC genomics 15, 166.

Gutierrez, A.P., Lubieniecki, K.P., Davidson, E.A., Lien, S., Kent, M.P., Fukui, S., Withler, R.E., Swift, B., Davidson, W.S., 2012. Genetic mapping of quantitative trait loci (QTL) for body-weight in Atlantic salmon (*Salmo salar*) using a 6.5 K SNP array. Aquaculture 358, 61-70.

Hanson, T., Sites, D., 2012. 2011 US catfish database. Fisheries.

Houston, R.D., Taggart, J.B., Cezard, T., Bekaert, M., Lowe, N.R., Downing, A., Talbot, R., Bishop, S.C., Archibald, A.L., Bron, J.E., Penman, D.J., Davassi, A., Brew, F., Tinch, A.E., Gharbi, K., Hamilton, A., 2014. Development and validation of a high density SNP genotyping array for Atlantic salmon (*Salmo salar*). BMC genomics 15, 90.

Jiang, Y., Gao, X., Liu, S., Zhang, Y., Liu, H., Sun, F., Bao, L., Waldbieser, G., Liu, Z., 2013. Whole genome comparative analysis of channel catfish (*Ictalurus punctatus*) with four model fish species. BMC genomics 14, 780.

Kucuktas, H., Wang, S., Li, P., He, C., Xu, P., Sha, Z., Liu, H., Jiang, Y., Baoprasertkul, P., Somridhivej, B., Wang, Y., Abernathy, J., Guo, X., Liu, L., Muir, W., Liu, Z., 2009. Construction of genetic linkage maps and comparative genome analysis of catfish using gene-associated markers. Genetics 181, 1649-1660.

Lien, S., Gidskehaug, L., Moen, T., Hayes, B.J., Berg, P.R., Davidson, W.S., Omholt, S.W., Kent, M.P., 2011. A dense SNP-based linkage map for Atlantic salmon (*Salmo salar*) reveals extended chromosome homeologies and striking differences in sex-specific recombination patterns. BMC genomics 12, 615.

Liu, H., Jiang, Y., Wang, S., Ninwichian, P., Somridhivej, B., Xu, P., Abernathy, J., Kucuktas, H., Liu, Z., 2009. Comparative analysis of catfish BAC end sequences with the zebrafish genome. BMC genomics 10, 592.

Liu, S., Sun, L., Li, Y., Sun, F., Jiang, Y., Zhang, Y., Zhang, J., Feng, J., Kaltenboeck, L., Kucuktas, H., Liu, Z., 2014. Development of the catfish 250K SNP array for genome-wide association studies. BMC research notes 7, 135.

Liu, S., Zhou, Z., Lu, J., Sun, F., Wang, S., Liu, H., Jiang, Y., Kucuktas, H., Kaltenboeck, L.,

Peatman, E., Liu, Z., 2011. Generation of genome-scale gene-associated SNPs in catfish for the construction of a high-density SNP array. BMC genomics 12, 53.

Liu, Z., Karsi, A., Li, P., Cao, D., Dunham, R., 2003. An AFLP-based genetic linkage map of channel catfish (*Ictalurus punctatus*) constructed by using an interspecific hybrid resource family. Genetics 165, 687-694.

Lorenz, S., Brenna-Hansen, S., Moen, T., Roseth, A., Davidson, W.S., Omholt, S.W., Lien, S., 2010. BAC-based upgrading and physical integration of a genetic SNP map in Atlantic salmon. Animal genetics 41, 48-54.

McCue, M.E., Bannasch, D.L., Petersen, J.L., Gurr, J., Bailey, E., Binns, M.M., Distl, O., Guerin, G., Hasegawa, T., Hill, E.W., Leeb, T., Lindgren, G., Penedo, M.C.T., Roed, K.H., Ryder, O.A., Swinburne, J.E., Tozaki, T., Valberg, S.J., Vaudin, M., Lindblad-Toh, K., Wade, C.M., Mickelson, J.R., 2012. A High Density SNP Array for the Domestic Horse and Extant Perissodactyla: Utility for Association Mapping, Genetic Diversity, and Phylogeny Studies. PLoS genetics 8, e1002451.

McPherson, J.D., Marra, M., Hillier, L., Waterston, R.H., Chinwalla, A., Wallis, J., Sekhon, M., Wylie, K., Mardis, E.R., Wilson, R.K., 2001. A physical map of the human genome. Nature 409, 934-941.

Miller, M.R., Dunham, J.P., Amores, A., Cresko, W.A., Johnson, E.A., 2007. Rapid and cost-effective polymorphism identification and genotyping using restriction site associated DNA (RAD) markers. Genome research 17, 240-248.

Myers, S., Bottolo, L., Freeman, C., McVean, G., Donnelly, P., 2005. A fine-scale map of recombination rates and hotspots across the human genome. Science 310, 321-324.

Ninwichian, P., Peatman, E., Liu, H., Kucuktas, H., Somridhivej, B., Liu, S., Li, P., Jiang, Y., Sha,

Z., Kaltenboeck, L., Abernathy, J.W., Wang, W., Chen, F., Lee, Y., Wong, L., Wang, S., Lu, J., Liu, Z., 2012. Second-generation genetic linkage map of catfish and its integration with the BAC-based physical map. G3:Genes| Genomes| Genetics 2, 1233-1241.

Palaiokostas, C., Bekaert, M., Khan, M.G.Q., Taggart, J.B., Gharbi, K., McAndrew, B.J., Penman, D.J., 2013. Mapping and Validation of the Major Sex-Determining Region in Nile Tilapia (*Oreochromis niloticus L*.) Using RAD Sequencing. PloS one 8, e68389.

Palti, Y., Genet, C., Gao, G., Hu, Y., You, F.M., Boussaha, M., Rexroad, C.E., 3rd, Luo, M.C., 2012. A second generation integrated map of the rainbow trout (*Oncorhynchus mykiss*) genome: analysis of conserved synteny with model fish genomes. Marine biotechnology 14, 343-357.

Quiniou, S.M., Waldbieser, G.C., Duke, M.V., 2007. A first generation BAC-based physical map of the channel catfish genome. BMC genomics 8, 40.

Rexroad, C.E., Palti, Y., Gahr, S.A., Vallejo, R.L., 2008. A second generation genetic map for rainbow trout (*Oncorhynchus mykiss*). BMC genetics 9, 74.

Song, W., Li, Y., Zhao, Y., Liu, Y., Niu, Y., Pang, R., Miao, G., Liao, X., Shao, C., Gao, F., Chen, S., 2012. Construction of a high-density microsatellite genetic linkage map and mapping of sexual and growth-related traits in half-smooth tongue sole (*Cynoglossus semilaevis*). PloS one 7, e52097.

Sun, L., Liu, S., Wang, R., Jiang, Y., Zhang, Y., Zhang, J., Bao, L., Kaltenboeck, L., Dunham, R., Waldbieser, G., Liu, Z., 2014. Identification and analysis of genome-wide SNPs provide insight into signatures of selection and domestication in catfish. PloS one 10, e109666.

Waldbieser, G.C., Bosworth, B.G., Nonneman, D.J., Wolters, W.R., 2001. A microsatellite-based genetic linkage map for channel catfish, *Ictalurus punctatus*. Genetics 158, 727-734.

Wang, C.M., Bai, Z.Y., He, X.P., Lin, G., Xia, J.H., Sun, F., Lo, L.C., Feng, F., Zhu, Z.Y., Yue, G.H., 2011. A high-resolution linkage map for comparative genome analysis and QTL fine mapping in Asian seabass, *Lates calcarifer.* BMC genomics 12, 174.

Xu, P., Wang, S., Liu, L., Thorsen, J., Kucuktas, H., Liu, Z., 2007. A BAC-based physical map of the channel catfish genome. Genomics 90, 380-388.

Zhang, Y., Liu, S., Lu, J., Jiang, Y., Gao, X., Ninwichian, P., Li, C., Waldbieser, G., Liu, Z., 2013. Comparative genomic analysis of catfish linkage group 8 reveals two homologous chromosomes in zebrafish and other teleosts with extensive inter-chromosomal rearrangements. BMC genomics 14, 387.

Zhao, L., Zhang, Y., Ji, P., Zhang, X., Zhao, Z., Hou, G., Huo, L., Liu, G., Li, C., Xu, P., Sun, X., 2013. A dense genetic linkage map for common carp and its integration with a BAC-based physical map. PloS one 8, e63928.

CHAPTER II

LITERATURE REVIEW

History of genetic mapping

Genetics as a branch of science has a relative short history of less than 160 years. It started in the mid-1800s, when Gregor Johann Mendel conducted a series of experiments with inheritance of a number of traits in peas. Through observations of phenotypes and analysis of the distribution of phenotypes among individuals in different generations, Mendel established his groundbreaking principles of inheritance, the so-called Mendel's Laws, which included the law of segregation (the "First Law"), the law of independent assortment (the "Second Law"), and the law of dominance (the "Third Law"). The law of segregation stated that during gamete formation, the alleles for each gene segregate from each other so that each gamete carries only one allele for each gene; the law of independent assortment states that genes for different traits segregate independently during the formation of gametes; and the law of dominance states that some alleles are dominant while others are recessive, recessive alleles are masked by dominant alleles (Bateson and Mendel, 1909; Miko, 2008; Wilson, 1902). These principles of inheritance set the foundation for genetics. However, with what known today as genetic linkage, Mendel was only partially correct because genes next to each other most often do not segregate independently because of their linkage.

In 1905, William Bateson, Edith Rebecca Saunders and Reginald Punnett examined flower

color and pollen shape in sweet pea plants by performing crosses similar to those carried out by Gregor Mendel, but they observed severe deviations from the predicted Mendelian independent assortment ratios (Bateson et al., 1909). They hypothesized that there was coupling, or connection between the parental alleles for flower color and pollen shape, and this coupling resulted in observed deviation from independent assortment. By 1910, geneticist Thomas Hunt Morgan made similar discoveries with the fruit fly (*Drosophila melanogaster*), where he found that the trait of eye color was correlated or "connected" with the sex factor. By analysis of the phenotypic ratios of the traits (Morgan, 1910), he hypothesized that the two traits were "linked". Thus, the term of "genetic linkage" was born, i.e., when two genes are closely associated on the same chromosome, they do not assort independently as Mendel initially proposed in his law of independent assortment (Morgan, 1911). With this knowledge in place, Morgan's student, Alfred Sturtevant, developed the first linkage map.

Genetic linkage maps are developed by placing "genes" on chromosomes based on the distances among them. If two genes segregate absolutely independently, they are considered to be located on two separate chromosomes, i.e., the original Mendel's law of independent assortment. However, if two genes are on the same chromosome, they do not assort independently, rather they are linked and therefore, assort depending on the distances between them. The greater the distance between linked genes are, the greater the chance that non-sister chromatids would cross over in the region between the genes. Therefore, recombination rate between genes is used as a measurement of genetic distance. This original concept for the measurement of genetic distance between genes is the basis for construction of genetic linkage maps.

The entire history of genetic linkage analysis is a mirror of technologies for the detection of polymorphisms. In the earliest days, polymorphisms were detected at the level of phenotypes or

traits. It was only possible to detect linkage among simple traits at the phenotypic level due to the lack of molecular markers. The discovery of DNA in 1953 (Watson and Crick, 1953) allowed the start of genetic analysis at the DNA level. However, for over 20 years after the DNA was discovered, the progress of linkage analysis has been slow because it was difficult to analyze genomic DNA with very high molecular weight. Then it was the discovery of restriction endonucleases in 1973 that made molecular analysis possible. With restriction endonucleases, high molecular weight DNA can be digested into smaller pieces that can be readily examined for their polymorphism. Even faster advances were made possible by the invention of DNA sequencing technologies in 1977 (Maxam and Gilbert, 1977; Sanger et al., 1977) that allowed greater abilities for the detection of polymorphism at single nucleotide level. Thereafter for the following decade, then considered rapid progress was made in the area of linkage mapping through the use of DNA markers, mostly in the form of restriction fragment length polymorphisms (RFLP), the most popular marker system by mid-1980's. Then it came 1986, when PCR technology was invented. The coupling of DNA sequencing technologies with PCR technology allowed rapid progress in DNA marker technologies. In particular, the application of microsatellites allowed much progress in linkage mapping. For almost another decade and a half, linkage mapping was among the most hot research areas in genetics using various polymorphic DNA markers such as microsatellites, RFLP, rapid amplification of polymorphic DNA (RAPD), amplified fragment length polymorphism (AFLP), among many types of polymorphic markers. However, all these technologies were relatively slow, laborious, and costly, as compared to the current marker technologies.

Further progress in linkage mapping was limited by the lack of large numbers of polymorphic markers and automated technologies. Although single nucleotide polymorphism (SNP) was

discovered as early as 1970's, effective technologies were not available for efficient and cost-effective analysis of SNPs until the beginning of this century. Similarly, methodologies for identification of large numbers of SNPs were not available. It was only with the most recent advances in next generation sequencing (NGS), was it possible to identify SNPs at a genome scale in a cost-effective manner (Davey et al., 2011). Along with the availability of highly efficient genotype array platforms, development of high-density and high-resolution genetic linkage maps became possible.

Principles of genetic mapping

Genetic mapping is the procedure for the construction of a genetic map (Van Ooijen and Jansen, 2013). A genetic map is made with markers or genes in a linear arrangement on chromosomes with relative distances between them. In contrast to physical distances where the distances between markers are measured by the physical length between genes or markers in base pairs, genetic distances are measured by frequencies of recombination between markers during crossovers of homologous chromosomes. The basic principles of linkage mapping lie in the fact that the farther apart the two markers on the same chromosome, the more likely that recombination can happen between the two markers, and conversely, the closer the two markers, the less likely that recombination can happen between them.

As stated in Mendel's law of independent assortment, chromosomes assort randomly into gametes, thus the segregation of alleles of one gene is independent of alleles of another gene if they reside on different chromosomes. However, independent assortment does not apply to genes residing on the same chromosome, simply because they are physically linked together. Unless recombination occurs, alleles carried on the same chromatids go together as a "unit", and they are

said to be linked (Semagn et al., 2006).

For two genes located at different chromosomes, they are unlinked. The chance that A/B or a/b co-inherit to the offspring is 0.5. Increases of this chance indicate linkage. If aB and Ab did not appear in the parental cells, they were called recombinants due to recombination. Recombination is the process that, during meiosis, the chromosome often breaks and the rejoins with the homologue chromosome (indicated as crossover), resulting in the production of the new alleles, the recombinant alleles aB and Ab (Whitehouse, 1982). The greater the frequency of recombination between two genetic makers or genes, the further apart they are on the same chromosome, and when the recombinant frequency increases to 0.5, the two genes are independently assorted, reflecting that they are indefinitely distant--they are on different chromosomes.

The recombination frequency (also called recombination fraction) between two loci is defined as the ratio of the number of recombinants to the total number of gametes produced (Xu, 2013). Therefore the minimum recombination fraction is 0, indicating no recombinants (i.e., the two genes are absolutely linked together). Maximum recombination fraction is 0.5, indicating the genes are on different chromosomes.

Important concepts of genetic mapping

Linkage phase

Two types of gametes are generated following genes or alleles on the same chromosome:

If crossing over does not occur, the products are parental gametes.

If crossing over occurs, the products are recombinant gametes.

The two possible arrangements of alleles on the homologous chromosomes are referred to as linkage phase. The allelic composition of parental and recombinant gametes depends upon whether the original cross involved genes in coupling or repulsion phase (Semagn et al., 2006). In diploid species, the most prevalent gametes in a coupling phase are two dominant alleles or two recessive alleles linked on one chromosome. For repulsion phase, gametes containing one dominant allele linked with one recessive allele will be most abundant type.

The distribution of gamete types should allow the differentiation of parental types from the recombinant types. In general, the two most frequent types of gametes are parental types while the two least frequent types of gametes are recombinant. This is because recombinant gametes can never account for more than 50% of the gametes. In addition, by examination of the frequency of gametes, one can determine if the original cross was a coupling or repulsion phase cross, which is important for estimating linkage distances (Lake et al., 2003).

The LOD score

linkage maps are made based on the genetic distances between markers, and genetic distances are estimated based on the chances for recombination. When chances are in question, statistical significance must be in place to assure the confidence one would have on the map. In this context, one key concept in genetic linkage analysis is the LOD score [logarithm (base 10) of odds], which is the most commonly used statistic to test whether or not two loci are truly linked. This method was developed by Newton E. Morton (Morton, 1955), which is an iterative approach where a series of LOD scores are calculated from a number of proposed linkage distance. The LOD score compares the likelihood of obtaining the test data if the two loci are indeed linked, to the likelihood of observing the same data purely by chance. The LOD score is calculated from the formula below:

$$\text{LOD} = \log 10 \ \frac{\text{likelihood if the loci are linked}}{\text{likelihood if unlinked}} = \log 10 \ \frac{(1-\theta)^{NR} X\ \theta^{R}}{0.5^{(NR+R)}}$$

Where R denotes the number of recombinant offspring, NR denotes the number of non-recombinant offspring, θ denotes the recombinant fraction. In linkage analysis, LOD of more than 3 is considered strong support for linkage, as it indicates the linkage is 1,000 times more probable than no linkage. On the contrary, a LOD score less than -2 is required for linkage exclusion. However, this criterion should be modified depending on the type of species, complexity of traits, and number of genetic markers (Morton, 1955).

Mapping function

In linkage mapping, the distance between two genes is determined by their recombination faction. Map construction based on distance and order of genetic markers. However, is it difficult to use only recombination fraction as a linkage metrics, because recombination factions themselves are not additive. Consider the loci A, B and C. If the recombination fraction between A and B is 0.2 and between B and C is 0.4, the recombination fraction between A and C should not be 0.6, as the maximum should be 0.5. Therefore, recombination fraction between A and C in not equal to the sum of the recombination fractions AB and BC. Furthermore, the distance between AC depends on the existence of interference, which is the effect in which the occurrence of a crossover in a certain region reduces the probability of a crossover in the adjacent region (Kinghorn and van der Werf, 2000). In that case, mathematical transformations were called mapping function, with the most well-known ones being Haldane (Haldane, 1919) and Kosambi (Kosambi, 1943).

The Haldane function assumes that there is no interference (all crossovers occur independently of one another): $D = -1/2 \ln (1-2\theta)$. Whereas Kosambi map function allows the occurrence of interference: $D = 1/4 \ln [(1+2\theta) (1-2\theta)]$.

Where D represents the genetic map distance between two marker loci, and θ represents the recombination fraction. Mapping functions translate recombination fractions between two loci into a map distance in cM (centiMorgan). In theory, 1% of recombinants equal approximately to 1 cM. Both mapping functions act over the range $0 < \theta < 0.5$. From the practical point of view, the Kosambi's function has been more widely used because of its advantage over Haldane's function for interference. And studies reported that the Kosambi's distances are more accurate than Haldane's in a multi-point analysis of data (Huehn, 2010; Vinod, 2011).

Requirements for genetic mapping

Genetic mapping requires four elements: 1) Genetic markers, 2) genotyping platforms, 3) mapping families and 4) mapping software.

Genetic markers

For linkage map construction one should first decide the type of molecular markers. Some commonly used types of genetic markers are described as following.

RFLP: RFLP is a type of polymorphism that results from variation in the DNA sequence (single nucleotide changes, insertions and deletions, repeat length polymorphism) recognized by restriction enzymes, and can be assayed by Southern hybridization (Kruglyak, 1997). RFLP was first used as a tool for genetic analysis in 1974. In that study, linkage of temperature-sensitive mutations of adenovirus to specific restriction fragment length differences was used to locate the mutations on a physical map of the restriction fragments (Grodzicker et al., 1974). In 1980, Botstein et al., proposed the original concept for construction of genetic map using RPLPs (Botstein et al., 1980). The first RLFP map of human genome was reported in 1987, which based

on the pattern of inheritance of 403 polymorphic loci, including 393 RFLPs (Donis-Keller et al., 1987). RFLP analysis was the first DNA profiling technique inexpensive enough to see widespread applications, and made human molecular genetics a reality. The major strength of RFLP is codominant marker. In the past, RFLP markers have been popular in linkage mapping. However, RFLPs are often not very polymorphic, and the vast majority of point mutations and small sizes of insertions or deletions are hard to detect due to the low resolution of agarose gel electrophoresis. Moreover, the combined process of marker developing, probe labeling, DNA fragmentation, electrophoresis, blotting, hybridization, washing and autoradiography made the technique for RFLP time-consuming and laboriously (Liu and Cordes, 2004).

RAPD: RAPD is based on the amplification by the PCR of random DNA segments, using single primers or arbitrary nucleotide sequence (8-10-mer). The amplified DNA fragments, referred to as RAPD markers, are able to differentiate between genetically distinct individuals (Williams et al., 1992). RAPD offers many advantages as it require no DNA probes and sequence information for primer design, it involves no blotting or hybridization steps, a large number of loci and individual can be easily screened. Therefore, RAPD analysis appears to offer a cost- and time-effective alternative to restriction fragment-length polymorphism (RFLP) analysis (Penner et al., 1993). It has been widely used in genetic mapping studies. However, shortcomings of RAPD markers are also obvious. It is difficult to distinguish whether a DNA segment is amplified from a locus that is heterozygous or homozygous because nearly all RAPD markers are dominant. In addition, mismatches between the primer and the template (different DNA regions which have the same lengths and thus appear to be a single locus) made the results difficult to be interpreted. In addition, RAPD are subject to low reproducibility due to the low annealing temperature used in the PCR amplification (Liu and Cordes, 2004). All these difficulties have limited the application

of this marker.

AFLP: AFLP is a technique that is capable of producing multilocus and reliable fingerprints of genomes basing on the selective PCR amplification of restriction fragments from a total digest of genomic DNA (Vos et al., 1995). The unique feature of AFLP technique is the addition of adaptors of known sequence to DNA fragments generated by digestion, which allows for the subsequent PCR amplification of a subset of the total fragments for ease of separation by gel electrophoresis (Liu and Cordes, 2004). There are many advantages to AFLP when compared to RAPD and RFLP methods discussed above. It has higher reproducibility, resolution and sensitivity at the whole genome level (Mueller and Wolfenbarger, 1999). In addition, it allows for the specific amplification and analyzed of high numbers of restriction fragments simultaneously instead of analyzing one locus at a time. Like RAPDs, it does not require any prior sequence information for amplification. As a result, AFLPs have emerged as a replacement of RAPDs and AFLPs are also as good choice for genetic mapping for organisms with barely genomic information. Unfortunately AFLP technique also has its weaknesses. The main disadvantage is just like RAPD markers, AFLP markers suffer from their general dominant nature, rendering this method less useful for studies that require precise assignment of allelic states (Mueller and Wolfenbarger, 1999).

Microsatellites: Microsatellites, also known as simple sequence repeats (SSR), are stretches of a short, tandemly repeated DNA motif (1-6 bp). Microsatellites are highly polymorphic with respect to motif reiterations due to their inherent mutation mechanism (Ellegren, 2004). There are several advantages of microsatellites marker over the other genetic markers. The primary advantage is that they are inherited in a Mendelian fashion as codominant markers. Moreover, they are selectively neutral because they randomly distribute throughout the genome. Furthermore,

high polymorphism rates, high abundance and a broad distribution have made microsatellites as ideal markers for genetic mapping (Hearne et al., 1992). Many successive genetic maps in humans have been constructed based mainly on this type of marker (Dib et al., 1996; Murray et al., 1994; Weissenbach et al., 1992). However, significant drawbacks do exist with respect to using microsatellite-based methods, including the necessity to know sequence information, relatively high development costs and technical challenges during the construction of enriched libraries and species-specific primers (Miah et al., 2013).

SNPs: After a whole decade of domination in the molecular genetics field for genomics and genetics studies by the microsatellite markers, a new marker type, named SNP, for Single Nucleotide Polymorphism, is now on the scene and has rapidly become the marker of choice for many applications. A SNP is a DNA sequence variation occurring when a single nucleotide in the genome differs between members of a species or between paired chromosomes in an individual (Srivastava and Mishra, 2009). SNP is becoming a focal point due to its potential for high genotyping efficiency, automation, data quality, genome-wide coverage and analytical simplicity (Davey et al., 2011; Frazer et al., 2009). Prior to the emergence of next-generation sequencing (NGS) technologies, the identification of SNPs has been fueled by mining large numbers of expressed sequence tags (ESTs) available in many species. However, it was severely limited by sequence coverage and depth (Liu et al., 2011). Now, the advent of next-generation sequencing technologies has revolutionized genomic and transcriptomic approaches to SNP discovery. Theoretically, SNPs may be bi-, three- and four-allelic; however, in practice even three-allelic SNPs are very rare (less than 0.1% of all human SNPs (Lai, 2001)). The overwhelming majority of SNPs are biallelic. There are four types of biallelic SNPs including one transition C/T (G/A), and three types of transversions: C/A (G/T), C/G (G/C) and T/A (A/T). The most abundant are

transitions, originating from the deamination of 5'-methylcytosine to thymine (Holliday and Grigg, 1993). The biallelic nature of SNPs leads to the lower polymorphism information content (PIC) value as compared to most other marker types which are often multiallelic (Kruglyak, 1997), but this shortcoming is greatly compensated by their high frequency.

SNP Genotyping platforms

With the availability of large numbers of SNPs, the challenge is how to genotype these SNPs efficiently and economically. The high-density SNP array platforms have been developed, which allow large-scale genotyping of SNPs in parallel in a large set of individuals (Syvanen, 2005). The BeadChip-based infinium assay (Illumina) (Oliphant et al., 2002), GoldenGate Genotying Technology (Illumina) (Fan et al., 2003), SNPStream (Beckman Coulter) (Bell et al., 2002), GeneChip (Affymetrix) (Dalma-Weiszhausz et al., 2006) and Affymetrix GeneChip Custom Array (Affymetrix, Santa Clara, CA) are widely used. These platforms differ in their requirements for sample size, SNP marker numbers, cost and automation (Liu et al., 2014). The appropriate platform for SNP genotyping needs to be chosen depends on specific project goals and budget levels. Alternatively, NGS-based genotyping by sequencing (GBS) (Baird et al., 2008; Davey et al., 2011b; Miller et al., 2007) is also highly efficient. GBS is widely used in numerous organisms, especially species lacking of prior genomic resources. Both SNP array and GBS have been used to genotype large-scale SNPs for genetic mapping and association analyses (Anderson et al., 2012; Everett et al., 2012; Gonen et al., 2014; Gutierrez et al., 2012; Houston et al., 2014). Compared to GBS, SNP arrays are more cost-effective. In addition, they provide a greater level of genome coverage. For instance, in most cases, the total number of commonly analyzed SNPs is limited to several thousand while millions of SNPs can be analyzed by using very high density SNP arrays. In addition, GBS of large resource panels for high resolution maps are cost-prohibitive.

Mapping families

The design of reference families is the foundation of a genetic mapping program because reference families affect the quality and cost of the linkage maps (Da et al., 1998). F1 families generated by crossing genetically diverse individuals, F2 populations derived from F1 hybrids, and backcross populations derived by crossing the F1 hybrid to one of the parents are the most commonly used types of mapping population for aquaculture species (Yue, 2013). Although some studies attempted to determine the ideal population size and type for constructing accurate maps (Ferreira et al., 2006; van der Beek et al., 1993), there are no standard rules for creating reference families. Based on previous experience, some universal comments that apply to any type of mapping population can be made as follows: 1) The amount of effective information available for mapping is based on the number of informative meiosis. In general, the informative meiosis means we can identify whether or not the gamete is recombinant. In practice, full-sib families are more efficient than half-sib families as full-sib family can yield more informative offspring. In that case, the requirement for the number of genotyping is lower for the same number of informative meiosis. 2) It is better to use more mapping families because one pair of parents may be homozygous at the locus that will not produce informative meiosis.3) The greater the number of individuals, the higher the map resolution is. In practice, although any number of individuals can be used, a large population size is needed for high-resolution mapping (van der Beek et al., 1993).

Linkage mapping software

There are a number of software packages available for linkage mapping. The detailed list of software for linkage mapping, QTL analysis and related studies can be found in website http://www.jurgott.org/linkage/ListSoftware.html. The type of software used is mainly dependent

on the experimental design, including the population structure and the number of genetic markers.

JoinMap (Stam, 1993), CRI-MAP (Green et al., 1990), MAPMAKER (Lincoln, 1992), LINKMFEX (Danzmann, 2001) and Map Manager QTX(Manly et al., 2001) for linkage map construction and MapChart (Voorrips, 2002) for map drawing are the most widely used tools in aquaculture species. As marker density becomes very high, which leads to the exponential increase in computational intensity (van Os et al., 2005), several new packages like OneMap (Margarido et al., 2007), MSTmap (Wu et al., 2008) and HighMap (Liu et al., 2014) have been developed for constructing high-density linkage maps. Each package has its own strengths and weaknesses. Therefore, it is wise to evaluate several software packages with genotype data before choosing a specific package for linkage analysis. It is also often productive to utilize combinations of software packages. For instance, using OneMap to place large numbers of markers into linkage groups, and then use JoinMap to order the markers and estimate their spacing.

Genetic map in aquaculture fish species

Genetic linkage maps have been constructed for a number of aquaculture species, such as Asian seabass (*Lates calcarifer*), Atlantic salmon (*Salmo salar*), Japanese flounder (*Paralichthys olivaceus*), channel catfish (*Ictalurus punctatus*), half-smooth tongue sole (*Cynoglossus semilaevis*) and common carp (*Cyprinus carpio*) (Castano-Sanchez et al., 2010; Cheng et al., 2010; Coimbra et al., 2003; Gilbey et al., 2004; Guyomard et al., 2012; Kocher et al., 1998; Kucuktas et al., 2009a; Lien et al., 2011b; Liu et al., 2003; Moen et al., 2008; Ninwichian et al., 2012; Sakamoto et al., 2000; Sun and Liang, 2004; Waldbieser et al., 2001; Wang et al., 2011; Wang et al., 2007). In the past decade, the relative high density genetic maps have been constructed in only a few species. The second generation linkage map of Asian seabass was spanned a genetic length of 2411.5 cM,

which harbored 790 microsatellite and SNP markers, with an average inter-marker distance of 3.4 cM or 1.1 Mb (Wang et al., 2011). The linkage map for Atlantic salmon was developed with a total of 5650 SNPs based on genotyping of 3297 fish from 143 families. The sex-specific map spanned a total of 2402.3 cM in female and 1746.2 cM in males, highlighting a difference in sex specific recombination rate 1.38 : 1(Lien et al., 2011). High-density genetic linkage map of half-smooth tongue sole were developed with 1007 microsatellite markers and two SCAR markers in 21 linkage groups, covering a total of 1624 cM with an average interval of 1.67 cM. The male map covered a total of 1447.3 cM and the female map spaned1497.5 cM (Song et al., 2012). 1124 microsatellite markers were mapped to 29 linkage groups of rainbow trout, covering a total of 2927.1 cM. The female having a map length of 4317.6 cM and the male map 2564.1 cM, with the female : male recombination ratio 1.68 : 1 (Rexroad et al., 2008). The genetic map of common carp contained 1209 genetic markers on 50 linkage groups, spanning 3565.9 cM on in genome (Zhao et al., 2013). Although these linkage maps provided a valuable resource for addressing important aquaculture, ecological, comparative genetics and evolutionary questions, only several hundred to thousand markers were mapped, with which QTL for agriculturally important performance and production traits can only be mapped in large genomic regions.

Genetic maps in channel catfish

For channel catfish, since the initiation of genome research over two decades ago, several genetic maps have been constructed with different types of molecular markers and various resource families.

One Microsatellite-based genetic linkage map for channel catfish was built using two reference families (two hundred full-sib offspring) in 2001, which harbored 293 microsatellite loci.

A total of 262 loci were placed into 32 multipoint linkage groups as LOD = 3.0 or greater, with an average of 171 informative meiosis per locus. These linkage groups range in length from 11.9 to 110.5 cM with the total length of 1958 cM. The overall recombination rate between female and male was 3.18-fold (Waldbieser et al., 2001).

In 2003, an AFLP-based genetic linkage map of channel catfish was constructed by using an interspecific hybrid resource family. The resource families were made by backcrossing the F1 hybrids of channel catfish females and blue catfish males. In this genetic map, a total of 418 AFLP markers were assigned to 44 linkage groups, which covered 1593 cM (Liu et al., 2003). Both the microsatellite-based and the AFLP-based linkage map constructed at that time showed nonequivalence between chromosome number and linkage groups produced. Obviously, more markers are needed to fill the gap to bring linkage groups belonging to the same chromosome number.

A genetic linkage map of channel catfish was built using EST-based microsatellite and SNP markers with interspecific family. In this map, 259 microsatellites and 72 SNPs were mapped to 29 linkage groups, which covered a genetic distance of 1811 cM with an average marker interval of 6.0 cM. The recombination rate for females was 1.6 times higher than that for males (Kucuktas et al., 2009). Although the number of linkage groups in this map equal to the chromosome number, this map harbor only a couple of hundred markers. In that case, high density linkage map are crucially important for further genetic studies.

The latest genetic map of catfish was reported in 2012, including 2099 BES (BAC-end sequence)-based microsatellites, 235 EST-derived microsatellites, 127 anonymous microsatellites, 17 next-generation sequence-based microsatellites and 79 SNPs. The total length of this map was approximately 2550 cM. The average number of mapped markers per linkage group was 63

markers, with an average intermarker distance of 1.4 cM (Ninwichian et al., 2012). This was a great improvement on the density and resolution of catfish genetic map. However, that work only anchored 44.8% of the catfish BAC physical map contigs, covering 52.8% of the genome.

Physical map

Genetic maps are based on the genetic linkage information measured in Centi-Morgans (CM), while physical maps use actual physical distances usually measured in number of base pairs. A physical map is a linear ordering of a set of clones encompassing one of more chromosomes. Physical maps are usually obtained by first digesting clones with restriction enzymes and then detecting the clone overlaps by matching the lengths of the fragments produced by digestion (Smith et al., 1987). Historically, several types of large-insert based physical maps have been used. These include YACs (Burke et al., 1987), BACs (McPherson et al., 2001), and Cosmid-based libraries (Eiglmeier et al., 1993). YACs have the largest capacity for cloning the large inserts, but they are relatively instable, and therefore their use in genome studies has been limited. Cosmid libraries have the smallest capacity for cloning the large inserts and therefore, their use in large insert libraries has also been limited. BACs are the most popular large insert libraries as they are stable, and can hold inserts of up to 200 kb. BAC-based physical maps can organize the entire genome into restriction fingerprints-based contigs. Such contigs are similar to the whole genome sequencing contigs, but are constructed using overlapping restriction enzyme fingerprints rather than overlapping sequences themselves for the whole genome sequence assemblies. By analysis of restriction fingerprints of overlapping genomic clones of BAC inserts, the whole genome can be organized into a limited number of contigs, most often in the thousands. A BAC-based physical map is important for the understanding of genome structure and organization and for position based

cloning of economically important genes. It can also provide a material and information basis for comparative mapping (Xu et al., 2007).

Because of their importance, physical maps have been constructed in several aquaculture fish species including Atlantic salmon (*Salmo salar*), Nile tilapia (*Oreochromis niloticus*), Medaka (*Oryzias latipes*), rainbow trout (*Oncorhynchus mykiss*) and channel catfish (Katagiri et al., 2005; Matsuda et al., 2001; Ng et al., 2005; Palti et al., 2009; Quiniou et al., 2007; Xu et al., 2007). In atlantic salmon (*Salmo salar*), a physical map was generated based on HindIII fingerprints of a publicly available BAC library. A total of 11.5 haploid genome equivalents (185,938 clones) were successfully fingerprinted. Contigs were first assembled via FPC using high-stringency, and then end-to-end joins yielded 4354 contigs and 37,285 singletons (Ng et al., 2005). A genome-wide physical map of the tilapia genome was constructed by restriction fingerprinting 35,245 BAC clones using high-resolution capillary polyacrylamide gel electrophoresis. The map consists of 3,621 contigs and is estimated to span 1.752 Gb in physical length (Katagiri et al., 2005). The first-generation physical map of the medaka genome in BAC clones contains 902 map segments that cover about 74% of the genome. The map contains 2721 markers which include a non-redundant set of 2328 loci from 2534 expressed sequences and 934 markers anchored to the medaka genetic map (Matsuda et al., 2001). The physical map of the rainbow trout (*Oncorhynchus mykiss*) was constructed by fingerprinting 192,096 BAC clones using the 4-color high-information content fingerprinting (HICF) method. The map consists of 4,173 contigs and 9,379 singletons. The total number of unique fingerprinting fragments (consensus bands) in contigs is 1,185,157, which corresponds to an estimated physical length of 2.0 Gb (Palti et al., 2012). In channel catfish, a BAC based physical map was generated using four-color fluorescence-based fingerprint. A total of 3,307 contigs, based on 30,582 BAC clones were assembled by FingerPrinted Contig software

(FPC) using a cutoff of 1X10-20. Each contig contains an average of 9.25 clones with and average size of 292 kb. The BAC-end-associated polymorphic markers would allow integration of the genetic and physical map (Xu et al., 2007).

Integrated map

Map integration is to place the same set of markers on both linkage and physical maps such that one can relate genetic map positions and physical sequence (Ninwichian et al., 2012). Integration of genetic map with physical map is useful for understanding genomes from different dimensions. The integrated map will be a possible framework for whole genome sequence assembly and is essential for comparative genome analysis, fine-scale QTL mapping and positional cloning of genes responsible for performance and production traits (Liu et al., 2009; Ninwichian et al., 2012). BAC-anchored genetic markers can be identified through BAC-end sequencing, and then the integrated map can be constructed by mapping of molecular markers from BAC-end sequences. Integrated maps have been developed in several aquaculture fish species using low-density genetic maps. In Atlantic salmon, BAC-anchored SNP markers were developed to enable the integration of physical and genetic maps by assigning 73 BAC contigs to Atlantic salmon linkage groups (Lorenz et al., 2010). The second generation of rainbow trout integrated map anchored up to 265 contigs to the genetic map, covering approximately 11% of the genome (Palti et al., 2012). In common carp, a total of 463 physical map contigs and 88 single BACs were integrated into the genetic linkage map, which covered 30% of the common carp genome (Zhao et al., 2013). In catfish, 2,030 BAC end sequence (BES)-derived microsatellites from 1,481 physical map contigs were used for linkage map construction, which anchored 44.8% of the catfish BAC physical map contigs, covering approximately 52.8% of the genome (Ninwichian et al., 2012).

Nowadays, BAC-based physical map construction and its integration with high-density genetic maps have benefited from NGS and high-throughput array platforms (Ariyadasa and Stein, 2012).

References

Anderson, J.L., Rodriguez Mari, A., Braasch, I., Amores, A., Hohenlohe, P., Batzel, P., Postlethwait, J.H., 2012. Multiple sex-associated regions and a putative sex chromosome in zebrafish revealed by RAD mapping and population genomics. PloS one 7, e40701.

Ariyadasa, R., Stein, N., 2012. Advances in BAC-based physical mapping and map integration strategies in plants. Journal of biomedicine research 2012, 1-11

Baird, N.A., Etter, P.D., Atwood, T.S., Currey, M.C., Shiver, A.L., Lewis, Z.A., Selker, E.U., Cresko, W.A., Johnson, E.A., 2008. Rapid SNP Discovery and Genetic Mapping Using Sequenced RAD Markers. PloS one 3, 10.

Bateson, W. 1902. Mendel's principles of heredity. University Press.

Bateson, W., Waunders, E., Punnett, R.C., 1909. Experimental studies in the physiology of heredity. Molecular and general genetics 2, 17-19.

Bell, P.A., Chaturvedi, S., Gelfand, C.A., Huang, C.Y., Kochersperger, M., Kopla, R., Modica, F., Pohl, M., Varde, S., Zhao, R., Zhao, X., Boyce-Jacino, M.T., Yassen, A., 2002. SNPstream UHT: ultra-high throughput SNP genotyping for pharmacogenomics and drug discovery. Biotechniques 32 (Suppl 2), S70-S77.

Botstein, D., White, R.L., Skolnick, M., Davis, R.W., 1980. Construction of a genetic linkage map in man using restriction fragment length polymorphisms. American journal of human genetics 32, 314.

Burke, D.T., Carle, G.F., Olson, M.V., 1987. Cloning of large segments of exogenous DNA into yeast by means of artificial chromosome vectors. Science 236, 806-812.

Castano-Sanchez, C., Fuji, K., Ozaki, A., Hasegawa, O., Sakamoto, T., Morishima, K., Nakayama, I., Fujiwara, A., Masaoka, T., Okamoto, H., Hayashida, K., Tagami, M., Kawai, J.,

Hayashizaki, Y., Okamoto, N., 2010. A second generation genetic linkage map of Japanese flounder (*Paralichthys olivaceus*). BMC genomics 11, 554.

Cheng, L., Liu, L., Yu, X., Wang, D., Tong, J., 2010. A linkage map of common carp (*Cyprinus carpio*) based on AFLP and microsatellite markers. Animal genetics 41, 191-198.

Coimbra, M.R., Kobayashi, K., Koretsugu, S., Hasegawa, O., Ohara, E., Ozaki, A., Sakamoto, T., Naruse, K., Okamoto, N., 2003. A genetic linkage map of the Japanese flounder, *Paralichthys olivaceus*. Aquaculture 220, 203-218.

Da, Y., VanRaden, P.M., Li, N., Beattie, C.W., Wu, C., Schook, L.B., 1998. Designs of reference families for the construction of genetic linkage maps. Animal biotechnology 9, 205-228.

Dalma-Weiszhausz, D.D., Warrington, J., Tanimoto, E.Y., Miyada, C.G., 2006. The affymetrix GeneChip platform: an overview. Methods in enzymology 410, 3-28.

Danzmann, R., 2001. LINKMFEX: Linkage analysis package for outcrossed mapping families with male or female exchange of the mapping parent. 2001.

Davey, J.W., Hohenlohe, P.A., Etter, P.D., Boone, J.Q., Catchen, J.M., Blaxter, M.L., 2011. Genome-wide genetic marker discovery and genotyping using next-generation sequencing. Nature reviews genetics 12, 499-510.

Dib, C., Faure, S., Fizames, C., Samson, D., Drouot, N., Vignal, A., Millasseau, P., Marc, S., Hazan, J., Seboun, E., Lathrop, M., Gyapay, G., Morissette, J., Weissenbach, J., 1996. A comprehensive genetic map of the human genome based on 5,264 microsatellites. Nature 380, 152-154.

Donis-Keller, H., Green, P., Helms, C., Cartinhour, S., Weiffenbach, B., Stephens, K., Keith, T.P., Bowden, D.W., Smith, D.R., Lander, E.S., et al., 1987. A genetic linkage map of the human genome. Cell 51, 319-337.

Eiglmeier, K., Honore, N., Woods, S., Caudron, B., Cole, S., 1993. Use of an ordered cosmid library to deduce the genomic organization of *Mycobacterium leprae.* Molecular microbiology 7, 197-206.

Ellegren, H., 2004. Microsatellites: simple sequences with complex evolution. Nature reviews. Genetics 5, 435-445.

Everett, M.V., Miller, M.R., Seeb, J.E., 2012. Meiotic maps of sockeye salmon derived from massively parallel DNA sequencing. BMC genomics 13, 521.

Fan, J.B., Oliphant, A., Shen, R., Kermani, B.G., Garcia, F., Gunderson, K.L., Hansen, M., Steemers, F., Butler, S.L., Deloukas, P., Galver, L., Hunt, S., McBride, C., Bibikova, M., Rubano, T., Chen, J., Wickham, E., Doucet, D., Chang, W., Campbell, D., Zhang, B., Kruglyak, S., Bentley, D., Haas, J., Rigault, P., Zhou, L., Stuelpnagel, J., Chee, M.S., 2003. Highly parallel SNP genotyping. Cold Spring Harbor symposia on quantitative biology 68, 69-78.

Ferreira, A., Silva, M.F.d., Cruz, C.D., 2006. Estimating the effects of population size and type on the accuracy of genetic maps. Genetics and molecular biology 29, 187-192.

Frazer, K.A., Murray, S.S., Schork, N.J., Topol, E.J., 2009. Human genetic variation and its contribution to complex traits. Nature reviews. Genetics 10, 241-251.

Gilbey, J., Verspoor, E., McLay, A., Houlihan, D., 2004. A microsatellite linkage map for Atlantic salmon (*Salmo salar*). Animal genetics 35, 98-105.

Gonen, S., Lowe, N.R., Cezard, T., Gharbi, K., Bishop, S.C., Houston, R.D., 2014. Linkage maps of the Atlantic salmon (*Salmo salar*) genome derived from RAD sequencing. BMC genomics 15, 166.

Green, P., Falls, K., Crooks, S., 1990. Documentation for CRI-MAP, version 2.4. Washington

University School of Medicine, St. Louis, MO.

Grodzicker, T., Williams, J., Sharp, P., Sambrook, J., 1974. Physical mapping of temperature-sensitive mutations of adenoviruses, Cold Spring Harbor Symposia on Quantitative Biology. Cold Spring Harbor Laboratory Press, 39, 439-446.

Gutierrez, A.P., Lubieniecki, K.P., Davidson, E.A., Lien, S., Kent, M.P., Fukui, S., Withler, R.E., Swift, B., Davidson, W.S., 2012. Genetic mapping of quantitative trait loci (QTL) for body-weight in Atlantic salmon (*Salmo salar*) using a 6.5 K SNP array. Aquaculture 358, 61-70.

Guyomard, R., Boussaha, M., Krieg, F., Hervet, C., Quillet, E., 2012. A synthetic rainbow trout linkage map provides new insights into the salmonid whole genome duplication and the conservation of synteny among teleosts. BMC genetics 13, 15.

Haldane, J., 1919.The combination of linkage values, and the calculation of distances between the loci of linked factors. J genet 8 (29), 299-309.

Hearne, C.M., Ghosh, S., Todd, J.A., 1992. Microsatellites for linkage analysis of genetic traits. Trends in genetics 8, 288-294.

Holliday, R., Grigg, G.W., 1993. DNA methylation and mutation. Mutation research 285, 61-67.

Houston, R.D., Taggart, J.B., Cezard, T., Bekaert, M., Lowe, N.R., Downing, A., Talbot, R., Bishop, S.C., Archibald, A.L., Bron, J.E., Penman, D.J., Davassi, A., Brew, F., Tinch, A.E., Gharbi, K., Hamilton, A., 2014. Development and validation of a high density SNP genotyping array for Atlantic salmon (*Salmo salar).* BMC genomics 15, 90.

Huehn, M., 2010. Random variability of map distances based on Kosambi's and Haldane's mapping functions. Journal of applied genetics 51, 27-31.

Katagiri, T., Kidd, C., Tomasino, E., Davis, J.T., Wishon, C., Stern, J.E., Carleton, K.L., Howe, A.E., Kocher, T.D., 2005. A BAC-based physical map of the Nile tilapia genome. BMC

genomics 6, 89.

Kinghorn, B., van der Werf, J., 2000. Identifying and incorporating genetic markers and major genes in animal breeding programs. Curso desarrollado en Belo Horizonte 31.

Kocher, T.D., Lee, W.-J., Sobolewska, H., Penman, D., McAndrew, B., 1998. A genetic linkage map of a cichlid fish, the tilapia (*Oreochromis niloticus*). Genetics 148, 1225-1232.

Kosambi, D., 1943. The estimation of map distances from recombination values. Annals of eugenics 12, 172-175.

Kruglyak, L., 1997. The use of a genetic map of biallelic markers in linkage studies. Nature genetics 17, 21-24.

Kucuktas, H., Wang, S., Li, P., He, C., Xu, P., Sha, Z., Liu, H., Jiang, Y., Baoprasertkul, P., Somridhivej, B., Wang, Y., Abernathy, J., Guo, X., Liu, L., Muir, W., Liu, Z., 2009. Construction of genetic linkage maps and comparative genome analysis of catfish using gene-associated markers. Genetics 181, 1649-1660.

Lai, E., 2001. Application of SNP technologies in medicine: lessons learned and future challenges. Genome research 11, 927-929.

Lake, S., Lyon, H., Tantisira, K., Silverman, E., Weiss, S., Laird, N., Schaid, D., 2003. Estimation and tests of haplotype-environment interaction when linkage phase is ambiguous. Human heredity 55, 56-65.

Lien, S., Gidskehaug, L., Moen, T., Hayes, B.J., Berg, P.R., Davidson, W.S., Omholt, S.W., Kent, M.P., 2011a. A dense SNP-based linkage map for Atlantic salmon (*Salmo salar*) reveals extended chromosome homeologies and striking differences in sex-specific recombination patterns. BMC genomics 12, 615.

Lincoln, S., 1992. Mapping genes controlling quantitative traits with MAPMAKER/QTL 1.1.

Whitehead Institute Technical Report.

Liu, D., Ma, C., Hong, W., Huang, L., Liu, M., Liu, H., Zeng, H., Deng, D., Xin, H., Song, J., 2014. Construction and Analysis of High-Density Linkage Map Using High-Throughput Sequencing Data. PloS one 9, e98855.

Liu, H., Jiang, Y., Wang, S., Ninwichian, P., Somridhivej, B., Xu, P., Abernathy, J., Kucuktas, H., Liu, Z., 2009. Comparative analysis of catfish BAC end sequences with the zebrafish genome. BMC genomics 10, 592.

Liu, S., Sun, L., Li, Y., Sun, F., Jiang, Y., Zhang, Y., Zhang, J., Feng, J., Kaltenboeck, L., Kucuktas, H., Liu, Z., 2014. Development of the catfish 250K SNP array for genome-wide association studies. BMC research notes 7, 135.

Liu, S., Zhou, Z., Lu, J., Sun, F., Wang, S., Liu, H., Jiang, Y., Kucuktas, H., Kaltenboeck, L., Peatman, E., Liu, Z., 2011. Generation of genome-scale gene-associated SNPs in catfish for the construction of a high-density SNP array. BMC genomics 12, 53.

Liu, Z., Cordes, J., 2004. DNA marker technologies and their applications in aquaculture genetics. Aquaculture 238, 1-37.

Liu, Z., Karsi, A., Li, P., Cao, D., Dunham, R., 2003. An AFLP-based genetic linkage map of channel catfish (*Ictalurus punctatus*) constructed by using an interspecific hybrid resource family. Genetics 165, 687-694.

Lorenz, S., Brenna-Hansen, S., Moen, T., Roseth, A., Davidson, W.S., Omholt, S.W., Lien, S., 2010. BAC-based upgrading and physical integration of a genetic SNP map in Atlantic salmon. Animal genetics 41, 48-54.

Manly, K.F., Cudmore Jr, R.H., Meer, J.M., 2001. Map Manager QTX, cross-platform software for genetic mapping. Mammalian genome 12, 930-932.

Margarido, G., Souza, A., Garcia, A., 2007. OneMap: software for genetic mapping in outcrossing species. Hereditas 144, 78-79.

Matsuda, M., Kawato, N., Asakawa, S., Shimizu, N., Nagahama, Y., Hamaguchi, S., Sakaizumi, M., Hori, H., 2001. Construction of a BAC library derived from the inbred Hd-rR strain of the teleost fish, *Oryzias latipes*. Genes and genetic systems 76, 61-63.

Maxam, A.M., Gilbert, W., 1977. A new method for sequencing DNA. Proceedings of the National academy of sciences 74, 560-564.

McPherson, J.D., Marra, M., Hillier, L., Waterston, R.H., Chinwalla, A., Wallis, J., Sekhon, M., Wylie, K., Mardis, E.R., Wilson, R.K., 2001. A physical map of the human genome. Nature 409, 934-941.

Miah, G., Rafii, M.Y., Ismail, M.R., Puteh, A.B., Rahim, H.A., Islam, K.N., Latif, M.A., 2013. A review of microsatellite markers and their applications in rice breeding programs to improve blast disease resistance. International journal of molecular sciences 14, 22499-22528.

Miko, I., 2008. Gregor Mendel and the principles of inheritance. Nature education 1, 134.

Miller, M.R., Dunham, J.P., Amores, A., Cresko, W.A., Johnson, E.A., 2007. Rapid and cost-effective polymorphism identification and genotyping using restriction site associated DNA (RAD) markers. Genome research 17, 240-248.

Moen, T., Hayes, B., Baranski, M., Berg, P.R., Kjøglum, S., Koop, B.F., Davidson, W.S., Omholt, S.W., Lien, S., 2008. A linkage map of the Atlantic salmon (*Salmo salar*) based on EST-derived SNP markers. BMC genomics 9, 223.

Morgan, T.H., 1910. Sex limited inheritance in Drosophila. Science 32, 120-122.

Morgan, T.H., 1911. Random segregation versus coupling in Mendelian inheritance. Science 34, 384.

Morton, N.E., 1955. Sequential tests for the detection of linkage. The American journal of human genetics 7, 277-318.

Mueller, U.G., Wolfenbarger, L.L., 1999. AFLP genotyping and fingerprinting. Trends in ecology and evolution 14, 389-394.

Murray, J.C., Buetow, K.H., Weber, J.L., Ludwigsen, S., Scherpbier-Heddema, T., Manion, F., Quillen, J., Sheffield, V.C., Sunden, S., Duyk, G.M., et al., 1994. A comprehensive human linkage map with centimorgan density. Science 265, 2049-2054.

Ng, S.H., Artieri, C.G., Bosdet, I.E., Chiu, R., Danzmann, R.G., Davidson, W.S., Ferguson, M.M., Fjell, C.D., Hoyheim, B., Jones, S.J., de Jong, P.J., Koop, B.F., Krzywinski, M.I., Lubieniecki, K., Marra, M.A., Mitchell, L.A., Mathewson, C., Osoegawa, K., Parisotto, S.E., Phillips, R.B., Rise, M.L., von Schalburg, K.R., Schein, J.E., Shin, H., Siddiqui, A., Thorsen, J., Wye, N., Yang, G., Zhu, B., 2005. A physical map of the genome of Atlantic salmon, *Salmo salar*. Genomics 86, 396-404.

Ninwichian, P., Peatman, E., Liu, H., Kucuktas, H., Somridhivej, B., Liu, S., Li, P., Jiang, Y., Sha, Z., Kaltenboeck, L., Abernathy, J.W., Wang, W., Chen, F., Lee, Y., Wong, L., Wang, S., Lu, J., Liu, Z., 2012. Second-generation genetic linkage map of catfish and its integration with the BAC-based physical map. G3: Genes| Genomes| Genetics 2, 1233-1241.

Oliphant, A., Barker, D.L., Stuelpnagel, J.R., Chee, M.S., 2002. BeadArray technology: enabling an accurate, cost-effective approach to high-throughput genotyping. Biotechniques 32, 56-58.

Palti, Y., Genet, C., Gao, G., Hu, Y., You, F.M., Boussaha, M., Rexroad, C.E., 3rd, Luo, M.C., 2012. A second generation integrated map of the rainbow trout (*Oncorhynchus mykiss*) genome: analysis of conserved synteny with model fish genomes. Marine biotechnology 14, 343-357.

Palti, Y., Luo, M.-C., Hu, Y., Genet, C., You, F.M., Vallejo, R.L., Thorgaard, G.H., Wheeler, P.A., Rexroad, C.E., 2009. A first generation BAC-based physical map of the rainbow trout genome. BMC genomics 10, 462.

Penner, G., Bush, A., Wise, R., Kim, W., Domier, L., Kasha, K., Laroche, A., Scoles, G., Molnar, S., Fedak, G., 1993. Reproducibility of random amplified polymorphic DNA (RAPD) analysis among laboratories. Genome Research 2, 341-345.

Quiniou, S.M., Waldbieser, G.C., Duke, M.V., 2007. A first generation BAC-based physical map of the channel catfish genome. BMC genomics 8, 40.

Rexroad, C.E., 3rd, Palti, Y., Gahr, S.A., Vallejo, R.L., 2008. A second generation genetic map for rainbow trout (*Oncorhynchus mykiss*). BMC genetics 9, 74.

Sakamoto, T., Danzmann, R.G., Gharbi, K., Howard, P., Ozaki, A., Khoo, S.K., Woram, R.A., Okamoto, N., Ferguson, M.M., Holm, L.-E., 2000. A microsatellite linkage map of rainbow trout (*Oncorhynchus mykiss*) characterized by large sex-specific differences in recombination rates. Genetics 155, 1331-1345.

Sanger, F., Nicklen, S., Coulson, A.R., 1977. DNA sequencing with chain-terminating inhibitors. Proceedings of the National Academy of Sciences 74, 5463-5467.

Semagn, K., Bjørnstad, Å., Ndjiondjop, M., 2006. Principles, requirements and prospects of genetic mapping in plants. African journal of biotechnology 5, 25.

Smith, C.L., Econome, J.G., Schutt, A., Klco, S., Cantor, C.R., 1987. A physical map of the Escherichia coli K12 genome. Science 236, 1448-1453.

Song, W., Li, Y., Zhao, Y., Liu, Y., Niu, Y., Pang, R., Miao, G., Liao, X., Shao, C., Gao, F., Chen, S., 2012. Construction of a high-density microsatellite genetic linkage map and mapping of sexual and growth-related traits in half-smooth tongue sole (*Cynoglossus semilaevis*). PloS

one 7, e52097.

Srivastava, S., Mishra, N., 2009. Genetic markers-a cutting-edge technology in herbal drug research. Journal of chemical and pharmaceutical research 1, 1-18.

Stam, P., 1993. Construction of integrated genetic linkage maps by means of a new computer package: Join Map. The plant journal 3, 739-744.

Sun, X., Liang, L., 2004. A genetic linkage map of common carp (*Cyprinus carpio L.*) and mapping of a locus associated with cold tolerance. Aquaculture 238, 165-172.

Syvanen, A.C., 2005. Toward genome-wide SNP genotyping. Nature genetics 37 Suppl, S5-10.

van der Beek, S., Groen, A.F., van Arendonk, J.A., 1993. Evaluation of designs for reference families for livestock linkage mapping experiments. Animal biotechnology 4, 163-182.

Van Ooijen, J.W., Jansen, J., 2013. Genetic Mapping in Experimental Populations. Cambridge University Press.

van Os, H., Stam, P., Visser, R.G., van Eck, H.J., 2005. SMOOTH: a statistical method for successful removal of genotyping errors from high-density genetic linkage data. Theoretical and applied genetics. 112, 187-194.

Vinod, K., 2011. Kosambi and the genetic mapping function. Resonance 16, 540-550.

Voorrips, R., 2002. MapChart: software for the graphical presentation of linkage maps and QTLs. Journal of Heredity 93, 77-78.

Vos, P., Hogers, R., Bleeker, M., Reijans, M., Van de Lee, T., Hornes, M., Friters, A., Pot, J., Paleman, J., Kuiper, M., 1995. AFLP: a new technique for DNA fingerprinting. Nucleic acids research 23, 4407-4414.

Waldbieser, G.C., Bosworth, B.G., Nonneman, D.J., Wolters, W.R., 2001. A microsatellite-based genetic linkage map for channel catfish, *Ictalurus punctatus.* Genetics 158, 727-734.

Wang, C.M., Bai, Z.Y., He, X.P., Lin, G., Xia, J.H., Sun, F., Lo, L.C., Feng, F., Zhu, Z.Y., Yue, G.H., 2011. A high-resolution linkage map for comparative genome analysis and QTL fine mapping in Asian seabass, *Lates calcarifer.* BMC Genomics 12, 174.

Wang, C.M., Zhu, Z.Y., Lo, L.C., Feng, F., Lin, G., Yang, W.T., Li, J., Yue, G.H., 2007. A microsatellite linkage map of Barramundi, *Lates calcarifer*. Genetics 175, 907-915.

Watson, J.D., Crick, F.H., 1953. Molecular structure of nucleic acids. Nature 171, 737-738.

Weissenbach, J., Gyapay, G., Dib, C., Vignal, A., Morissette, J., Millasseau, P., Vaysseix, G., Lathrop, M., 1992. A second-generation linkage map of the human genome. Nature 359, 794-801.

Whitehouse, H.L., 1982. Genetic recombination. John Wiley and Sons.

Williams, J., Hanafey, M.K., Rafalski, J.A., Tingey, S.V., 1992. Genetic analysis using random amplified polymorphic DNA markers. Methods in enzymology 218, 704-740.

Wilson, E.B., 1902. Mendel's Principles of Heredity and the Maturation of the Germ-Cells. Science 16, 991-993.

Wu, Y., Bhat, P.R., Close, T.J., Lonardi, S., 2008. Efficient and accurate construction of genetic linkage maps from the minimum spanning tree of a graph. PLoS genetics 4, e1000212.

Xu, P., Wang, S., Liu, L., Thorsen, J., Kucuktas, H., Liu, Z., 2007. A BAC-based physical map of the channel catfish genome. Genomics 90, 380-388.

Xu, S., 2013. Principles of statistical genomics. New York : Springer.

Yue, G.H., 2013. Recent advances of genome mapping and marker‐assisted selection in aquaculture. Fish and fisheries 15, 376-396.

Zhao, L., Zhang, Y., Ji, P., Zhang, X., Zhao, Z., Hou, G., Huo, L., Liu, G., Li, C., Xu, P., Sun, X., 2013. A dense genetic linkage map for common carp and its integration with a BAC-based

physical map. PloS one 8, e63928.

♯ CHAPTER III

CONSTRUCTION OF A HIGH-DENSITY HIGH-RESOLUTION GENETIC MAP AND ITS INTEGRATION WITH BAC-BASED PHYSICAL MAP IN CHANNEL CATFISH

MATERIALS AND METHODS

Resource families and DNA preparation

A total of 576 fish, with 192 full-sib individuals from each of three full-sib channel catfish families, were used for linkage mapping. The parent and grandparent samples were also obtained. All DNA for these samples used in this study were provided by USDA-ARS Warmwater Aquaculture Research Unit which were prepared following the procedures as previous described (Waldbieser et al., 2001). In brief, the fish were euthanized with tricaine methanesulfonate (MS 222) at 300 mg/l before blood collection. For each individual, 500 μl blood samples were collected in a 1-ml syringe and immediately expelled into a 50-ml tube containing 20-ml of DNA extraction buffer (10 mM Tris, 100mM NaCl, pH8, 25 mM EDTA, 0.5% SDS, and freshly added proteinase K 0.1 mg.ml). Total DNA was isolated using the DNeasy Blood & Tissue Kit (Qiagen, Valencia, CA, USA) following the manufacturer's protocol.

♯ Published in DNA research

SNP genotyping

DNA samples were arranged in 96-well microtiter plates and diluted to a final concentration of 50 ng / µl with the final volume of 10 µl. Genotyping was conducted by GeneSeek (Lincoln, NE, USA) using the catfish 250K SNP array (Liu et al., 2014). Affymetrix CEL files were analyzed using Affymetrix Genotyping Console software (version 4.0) for quality control analysis and SNP genotype calling using the Affymetrix AxiomGT1 algorithm. Samples passing the quality control (Dish value > 0.85) and SNP call rates threshold (>95%) were retained for analysis. Following genotyping, an R package, SNPolisher, was used to generate the genotyping outputs. The package produced SNP quality control metrics and divided SNPs into several classes based on the quality of genotype calls (Liu et al., 2014). The polymorphic markers with high resolution of cluster separation (high genotyping quality) were remained for further analysis. The CHP files generated from the Affymetrix Genotyping Console were imported into SNP & Variation Suite (SVS version 7, Golden Helix Inc) for further filtering to remove SNPs with missing genotypes >10% and minor allele frequency <5%.

SNP filtering

For SNPs, only those had high quality of genotype calls and were heterozygous in at least one parent were retained for linkage analysis. Based on segregation patterns, SNPs were categorized into three types: 1:2:1 type (AB x AB, segregating in both parents), 1:1 type (AB x AA or AB x BB, segregating only in female), and 1:1 type (AA x AB or BB x AB, segregating only in male). The other types were removed initially because they are not informative for linkage mapping.

Markers with segregation distortion can also lead to inaccuracy in linkage mapping. In many cases, markers that are distorted significantly should not be used in the linkage mapping because

they could create inaccurate distances and false linkages (Cervera et al., 2001; Recknagel et al., 2013). In our study, the Chi-square goodness-of-fit tests were performed to examine the segregation distortion. Markers with significant segregation distortion were excluded ($P<0.001$).

It was also observed that genetic recombination rates could be artificially inflated when genotyping errors occur or when markers with large amounts of missing data are included in the analysis (Ronin et al., 2012; Ronin et al., 2010). Missing data can lead incorrect marker orders, especially in map regions with dense markers. Furthermore, it was reported that missing values tend to reduce the map lengths for widely separated markers, particular under the weighted least-squares criterion (Hackett and Broadfoot, 2003). In our case, SNPs with more than 10% missing values were removed before further analysis.

Linkage map construction

Assigning markers into linkage groups

Linkage maps were initially developed independently for the three mapping families. Sex-specific maps were constructed for each parent using 1:1 segregation type markers only (AB x AA or AB x BB for female map and AA x AB or BB x AB for male map). The markers of segregation type 1:2:1 (AB x AB) were used to build the sex-averaged map. The LINKMFEX software (version 2.4, http://www.uoguelph.ca/~rdanzman/software.htm) was used to perform linkage analysis for sex-specific markers and OneMap (R package, version 2.0) was used for linkage analysis of sex-averaged markers. Linkage between markers was examined by estimating LOD scores for recombination fraction (θ). In linkage analysis, LOD of more than 3 is considered strong support for linkage, as it indicates the linkage is 1,000 times more probable than no linkage. On the contrary, a LOD score less than -2 is required for linkage exclusion. However, this criterion should be modified depending on the type of species, complexity of traits, and number of genetic

markers. In our study, a LOD threshold of 8.0 was used, and a maximum θ of 0.35 was set to assign markers into linkage groups.

The availability of a large number of SNP markers and efficient SNP genotyping technology allow the construction of high-density linkage map. However a new problem arises. In many practical cases, the number of markers may exceed the resolution of recombination for the given population size, which lead to marker stacking, i.e., mapping of many markers to a single genetic location. In this study, for markers falling into 'zero recombination clusters', only one marker was picked which had the most informative meiosis as the "representative marker" of each cluster for linkage map construction in order to reduce the power required for computation of linkage. After building the map with "representative markers", the stacked markers with "zero recombination clusters" that were excluded during the initial mapping steps should be relocated onto the linkage maps based on the positions of their representative anchor marker. Such stacked markers are still valuable for the chromosome-scale scaffolding of genomic sequence.

Ordering markers within each linkage group

Map ordering in each group were constructed using JoinMap software version 4.0 with the regression mapping algorithm (Van Ooijen, 2006). The positions of markers were determined according to the sequential buildup of the map (Stam, 1993). First, the most informative pair of markers was selected, followed by adding other loci one by one. The best position of newly added marker was searched by comparing the goodness-of-fit test (Chi-square) of the calculated map for each tested position. A big normalized difference in goodness-of-fit Chi-square before and after adding a locus (jump) indicated a poor fit of the added marker. When the newly-added marker caused large jump or negative distance estimated in the map, the marker was removed. This procedure was repeated until all loci were tested once (first round). Some markers that have been

removed in the first round would be added to the map in the second round, however, the markers that produce too large a jump or negative distances should still not be used. In the third round, all markers previously removed were forced to add into the map without constraints of maximum allowed jump and no negative distances. In that case the results from the third round should not be considered as a map of high quality because some poor-fitting loci still exist. In that case, we only use the ordering results from the second round.

Determining the map distance

In linkage mapping, the distance between two genes is determined by their recombination faction. Map construction based on distance and order of genetic markers. However, is it difficult to use only recombination fraction as a linkage metrics, because recombination factions themselves are not additive. Furthermore, the distance depends on the existence of interference, which is the effect in which the occurrence of a crossover in a certain region reduces the probability of a crossover in the adjacent region (Kinghorn and van der Werf, 2000). In that case, mathematical transformations were called mapping function, with the most well-known ones being Haldane (Haldane, 1919) and Kosambi (Kosambi, 1943). Mapping functions translate recombination fractions between two loci into a map distance in cM (centiMorgan). We chose the Kosambi mapping function to convert the recombination frequencies into map distances (centiMorgans) because of its advantage over Haldane's function for interference. For the sex-specific markers, the linkage phases were inferred automatically, while for the markers with 1:2:1 segregation type (AB x AB), the linkage phase was deduced based on the genotypes of grandparents to assist the map construction.

Constructing the consensus maps

The consensus maps were then established using the MergeMap (Wu et al., 2011) by

integrating individual maps from three reference families through shared markers. In brief, the individual genetic maps were given as directed acyclic graphs (DAGs) internally, which were then merged into a consensus graph on the basis of shared vertices. Cycles in the consensus graph indicated ordering conflicts among the individual maps. Conflicts were resolved using a parsimonious approach that takes into account two types of errors that may be present in the individual maps, namely, local reshuffles and global displacements. Local reshuffles referred to inaccuracies in the order of nearby markers, whereas global displacements referred to the cases where a few markers were placed at wrong positions far from the correct ones. MergeMap resolved conflicts by deleting a minimum set of marker occurrences. To use MergeMap, map files of each individual genetic linkage map and a configuration file in the following format were needed. The configuration file was like following format: map1_name map1_weight map1_path. The weight represented the user's confidence in the quality of the map (High weight was associated with high quality). When MergeMap tried to resolve conflict, the minimum-weight set of marker occurrences were deleted. The following command was executed to construct the consensus map: Consensus_map.exe configuration_file.

Four output files were generated after running the MergeMap command. There were three graphs in the .dot format (lgx.dot, lgx_consensus.dot and lgx_linear.dot) and one text file showing the final consensus map. The lgx.dot graph highlighted the conflicts among the individual maps and showed the solution by MergeMap as to which marker occurrence was deleted. The lgx_consensus.dot showed the simplified consensus DAG, while the lgx_linear.dot showed the final linear consensus map.

Lastly, the markers falling into “zero recombination clusters” that were excluded during map construction were anchored to the linkage map based on the positions of their corresponding

representative markers.

Drawing linkage maps

All genetic linkage maps were drawn using MAPCHART 2.2 (Voorrips, 2002). MapChart read the linkage information (i.e. the locus and their positions) from text files, which were created with JoinMap. The text containing the map data specified the order of linkage groups. Each linkage group specification consisted of a header line followed by a loci section.

Differences in recombination rates between families and sexes

To assess differences in recombination rates among the three resource families, the sex-averaged map was used following the M-test according to Ott's method (Ott, 1999).

$$X^2 = 2 \times \ln(10)[\sum Z_i\left(\hat{\theta}_i\right) - Z(\hat{\theta})]$$

Where $Z_i(\hat{\theta}_i)$ represents the LOD scores of maximum likelihood estimation (MLE) for the ith reference family for common marker pairs among the three families. The $Z(\hat{\theta})$ represents the total LOD scores of MLE for all three families. The recombination fractions for all mapped locus intervals from each family were obtained from JoinMap.

To investigate sex-specific heterogeneity throughout each linkage group, common marker pairs were used to compare the locus intervals across the male-specific map and female-specific map using contingency G-test (Garcia-Dorado and Gallego, 1992).

Integration of linkage map with physical map

To integrate previously developed physical map (Xu et al., 2006) with the high-density linkage map constructed in the present work, all the mapped SNPs with 70-bp flanking sequences

were aligned with BAC end sequence (BES) (Liu et al., 2009; Xu et al., 2006) and BAC-based physical map contig-specific sequences (PMCSS) (Jiang et al., 2013) using BLAST with the E-value cutoff of 1E-10, minimal alignment length of 36 and minimal identity of 95%. The relationship of physical map and genetic map was built up based on the SNP associated BES and PMCSS. The BAC physical map contigs that harbored BAC-derived BES and PMCSS were anchored onto the genetic map based on the SNP positions.

RESULTS

Selection of SNP markers

SNP genotypes were obtained from 576 samples of three mapping families (192 samples per family). According to the assessment of genotyping quality and polymorphism in all samples from the three mapping families, genotypes of a total of 121,521 SNPs were used (Figure 1). Due to the low genotype calling rate (< 95%), nine individuals were excluded for analysis, including one individual from family 1, three individuals from family 2, and five individuals from family 3. After further filtering to remove SNPs with low calling rate (< 97%) and non-Mendelian inheritance ($P<0.001$), a total of 18,866 SNPs from family 1, 33,224 SNPs from family 2 and 35,093 SNPs from family 3, were retained for linkage mapping. Taken together, a total of 64,889 SNPs that were informative in at least one of the three mapping families were used. The SNPs filtering process was illustrated in Figure 1.

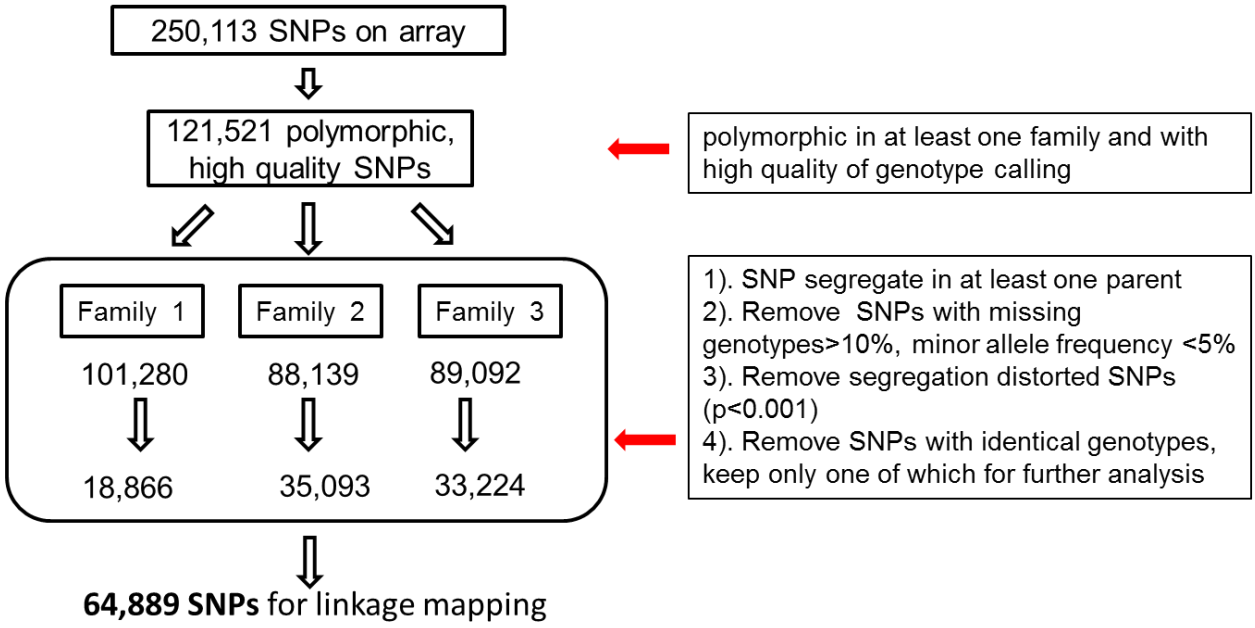

Figure 1. SNPs filtering process for linkage mapping

Linkage mapping

Linkage maps were first constructed for each of the three families, separately. For all three mapping families, 29 linkage groups (LGs) were obtained, which was consistent with the number of chromosomes of the catfish haploid genome. The consensus genetic linkage maps were obtained by merging separate maps from three mapping families. A total of 31,387 markers with unique genetic positions (hereafter referred to as unique markers) were placed on the consensus linkage maps, which included 8,644 SNPs from family 1, 13,477 SNPs from family 2 and 14,343 SNPs from family 3 (Table 1). After anchoring the previously excluded markers that fell into "zero

recombination clusters" based on the genetic positions of representative markers, a total of 54,342 SNP markers were placed onto the current linkage map (Table 1).

Table 1 - SNPs placed on the linkage maps

Item	Number
Unique SNPs from family 1 mapped to linkage map	8,644
Unique SNPs from family 2 mapped to linkage map	13,477
Unique SNPs from family 3 mapped to linkage map	14,343
Total unique SNPs mapped to linkage map	31,387
Total SNPs mapped to linkage map	54,342

The sex-specific maps were constructed using markers that were heterozygous in only female or male parent. The female genetic map consisted of 18,444 SNPs including 9,746 unique markers, with a total genetic length of 4,495.1 cM (Table 2, Fig. 2). The marker intervals estimated based on the unique marker positions ranged from 0.37 cM/marker pair in LG12 to 0.7 cM/marker pair in LG18 with the average marker interval of 0.46 cM/marker pair in female genetic map.

The male genetic map was comprised of 15,148 SNPs with 7,250 unique markers and a total genetic length of 2,593.7 cM, which was much shorter than female genetic map. The marker intervals of male genetic map ranged from 0.25 cM/marker pair (LG18) to 0.55 cM/marker pair (LG1), with an average marker interval of 0.36 cM (Table 3, Fig. 3). It should be noted that these distances refer to intervals where recombination was detected and of course it should be recognized that in both sexes the minimum distance observed was 0 cM for completely linked markers. The

female and male-specific maps were illustrated in Figure 2 and 3, respectively. The detailed map information was provided in Additional file 1.

Table 2 - Summary of the female linkage map of channel catfish

Linkage group	Female-specific map			
	Mapped markers	Unique positions	Genetic length (cM)	Marker interval (cM)
1	810	397	209.8	0.53
2	616	370	147.1	0.4
3	934	481	230.6	0.48
4	774	380	166.8	0.44
5	643	353	165.3	0.47
6	821	470	205.3	0.44
7	583	313	134.9	0.43
8	550	326	160.4	0.49
9	751	399	177.6	0.45
10	488	238	133.4	0.56
11	815	434	198.5	0.46
12	695	361	133.9	0.37
13	604	311	149.3	0.48
14	598	340	133.9	0.39
15	651	332	145.5	0.44
16	799	385	178.1	0.46
17	792	420	175.4	0.42
18	473	230	160.3	0.7
19	542	302	139.3	0.46
20	657	344	162.5	0.47
21	576	318	134.1	0.42
22	308	153	65.8	0.43
23	668	319	125.3	0.39
24	518	296	134.5	0.45
25	665	348	150.2	0.43
26	389	181	124.9	0.69
27	595	327	152.9	0.47
28	663	334	141.7	0.42
29	466	284	157.4	0.55
Total	**18,444**	**9,746**	**4,495.10**	**0.46**

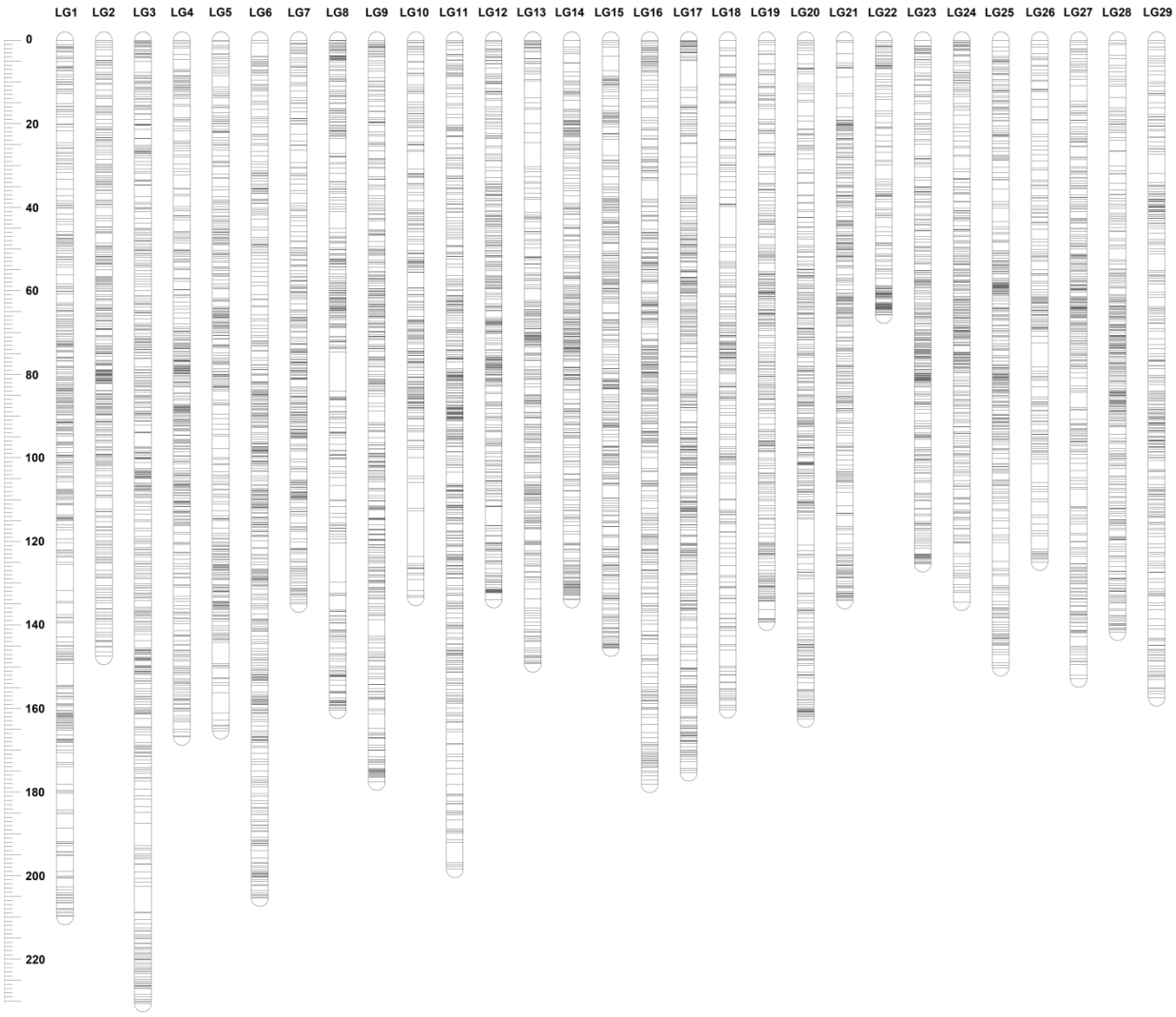

Figure 2 - Illustration of female-specific linkage map

Table 3 - Summary of the male-specific linkage maps of channel catfish

Linkage group	Male-specific map				F:M ratio
	Mapped markers	Unique positions	Genetic length (cM)	Marker interval (cM)	
1	374	153	83.9	0.55	2.50
2	517	251	90.6	0.36	1.62
3	665	342	126.4	0.37	1.82
4	699	313	110	0.35	1.52
5	441	199	79.1	0.40	2.09
6	606	300	132.1	0.44	1.55
7	370	196	63.1	0.32	2.14
8	615	297	92.7	0.31	1.73
9	546	291	97.1	0.33	1.83
10	516	228	75.7	0.33	1.76
11	616	273	111.6	0.41	1.78
12	727	311	82.2	0.26	1.63
13	557	285	123.6	0.43	1.21
14	351	150	79.2	0.53	1.69
15	524	248	73.8	0.30	1.97
16	635	337	111.2	0.33	1.60
17	506	264	103.6	0.39	1.69
18	640	290	73.5	0.25	2.18
19	495	256	95.9	0.37	1.45
20	557	244	88.2	0.36	1.84
21	437	217	76.4	0.35	1.76
22	380	169	67.9	0.40	0.97
23	478	245	73.9	0.30	1.70
24	408	195	72.6	0.37	1.85
25	535	269	109.3	0.41	1.37
26	512	242	76.9	0.32	1.62
27	522	233	70.4	0.30	2.17
28	484	237	80.5	0.34	1.76
29	435	215	72.5	0.34	2.17
Total	**15,148**	**7,250**	**2,593.7**	**0.36**	**1.73**

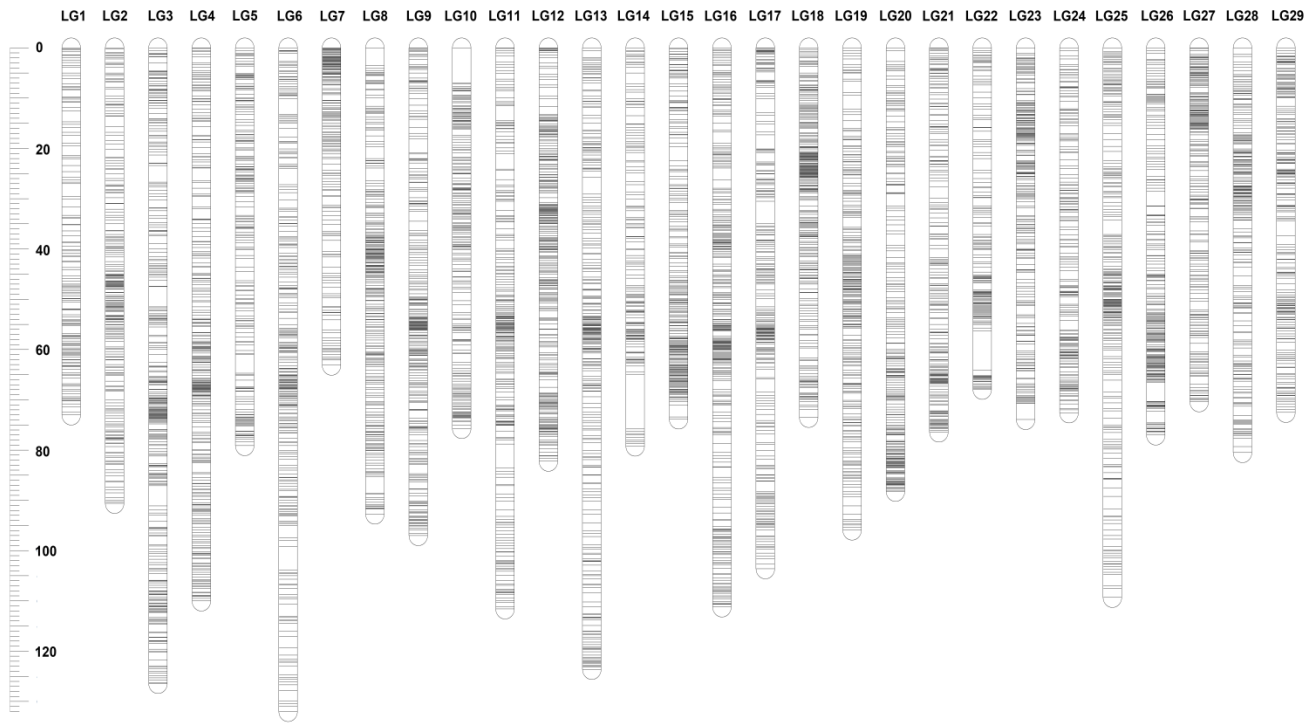

Figure 3 - Illustration of male-specific linkage map.

The sex-averaged map was constructed using markers that were heterozygous in both parents. As summarized in Table 4, a total of 29,081 SNPs were mapped, which consisted of 15,598 unique markers. The sex-averaged map spanned 3,505.4 cM with an average marker interval of 0.22 cM, ranging from 0.17 cM/marker (LG12) to 0.30 cM/marker (LG18). The genetic map was illustrated in Figure 4. The detailed map information was provided in Additional file 1 (Example shows on Table S1).

Table 4 - Summary of the sex-averaged linkage map of channel catfish

Linkage group	Sex-averaged map			
	Mapped markers	Unique positions	Genetic length (cM)	Marker interval (cM)
1	1,039	556	139.5	0.25
2	1,014	557	116.2	0.21
3	1,212	673	169.7	0.25
4	1,220	653	128.1	0.20
5	1,002	491	110.2	0.22
6	1,183	680	163.3	0.24
7	861	422	102.1	0.24
8	1,073	557	117.3	0.21
9	1,100	604	146.9	0.24
10	913	475	105.8	0.22
11	999	572	152.7	0.27
12	1,216	625	104.8	0.17
13	1,176	630	131.1	0.21
14	868	472	113.8	0.24
15	1,047	562	115.7	0.21
16	1,219	695	145.3	0.21
17	1,178	623	138.2	0.22
18	782	388	114.8	0.30
19	914	523	118.9	0.23
20	1,029	550	126	0.23
21	968	484	110.3	0.23
22	779	364	68.4	0.19
23	929	486	93.3	0.19
24	854	492	106.9	0.22
25	1,097	584	127.6	0.22
26	811	427	101.2	0.24
27	925	516	113.7	0.22
28	969	516	114.1	0.22
29	704	421	109.5	0.26
Total	**29,081**	**15,598**	**3,505.4**	**0.22**

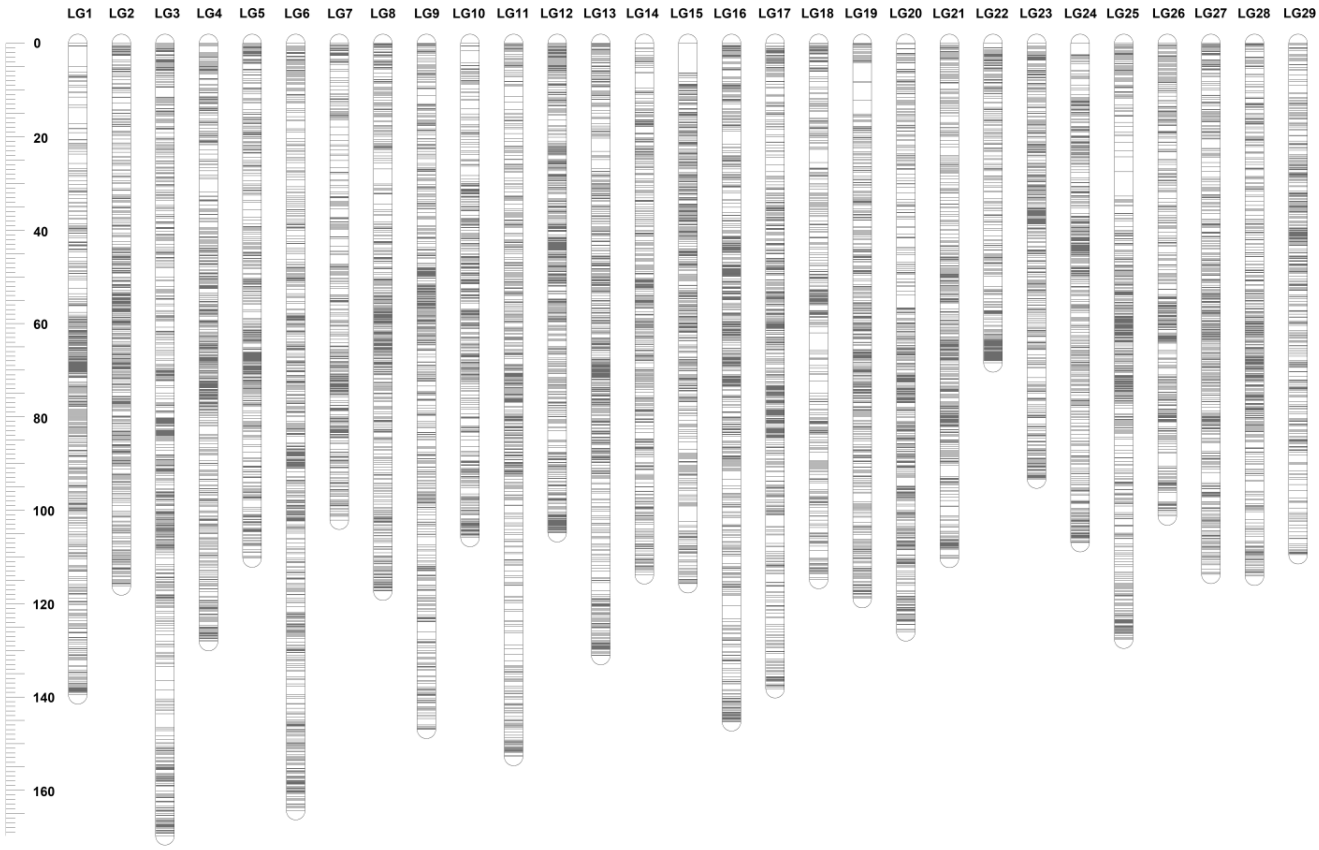

Figure 4 - Illustration of sex-averaged linkage map.

Analysis of recombination rates

Within each linkage group, mild to strong localized specific recombination pattern were observed, whereby recombination rates were usually elevated towards the end and suppressed in the middle of the map (Figure 5). Clustered markers that fell into “zero recombination rate” were observed in every linkage group, especially in positions close to the centromeres in contrast to the telomeres (Additional file 1).

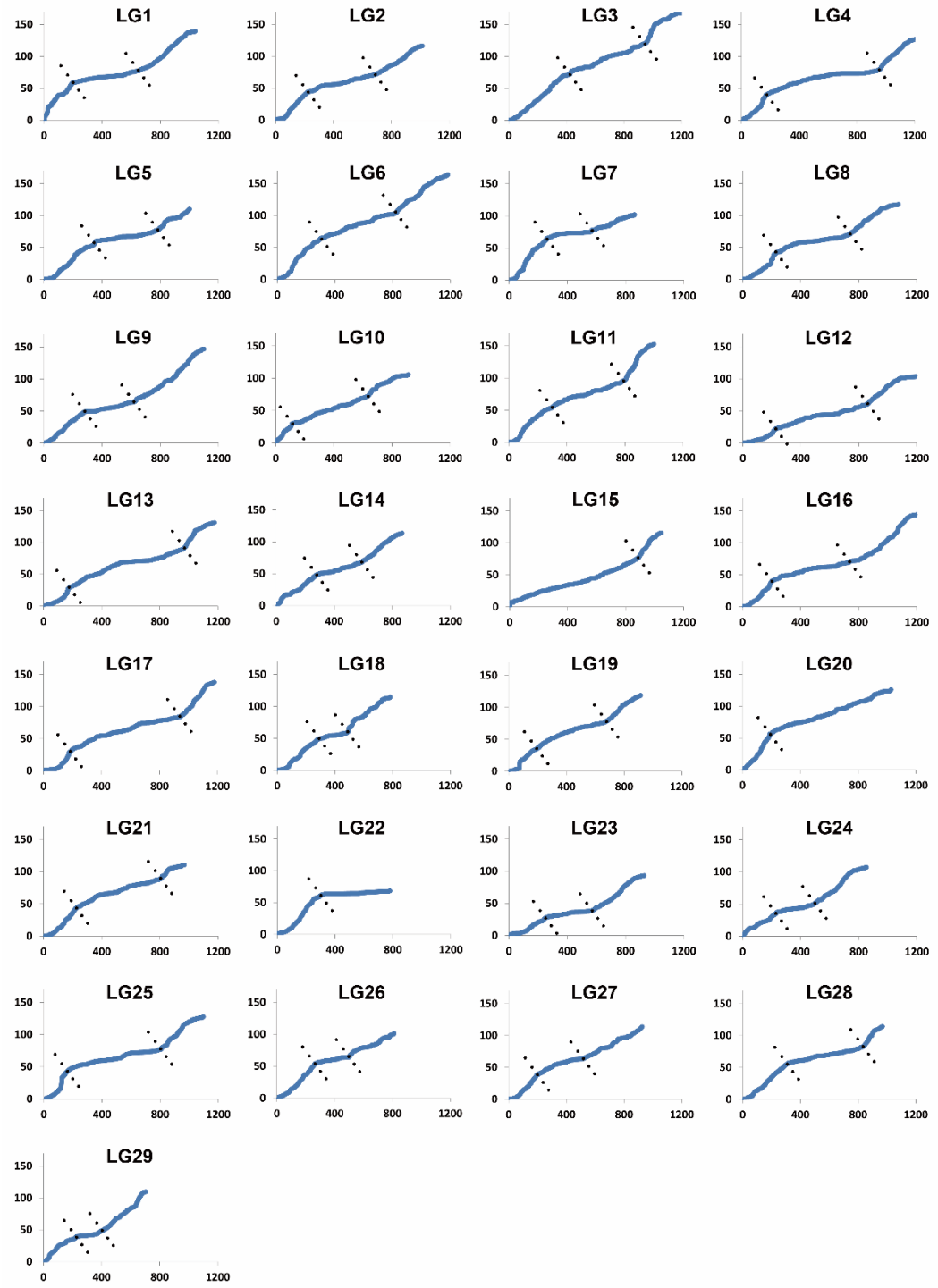

Figure 5 - The patterns of localized regional recombination rates along each linkage group.

There is no significant difference in recombination rate among three mapping families based on the examination with common marker pairs among the three families (see Methods section). In contrast, significant higher recombination rates were observed in a majority of the linkage groups of the female genetic map than that of male genetic map ($p < 0.01$). Overall, the female genetic map was 1,901.4 cM longer than male-genetic map, with an average female-to-male ratio of 1.7:1 (Table 3). The ratio varied by linkage groups, ranging from 0.97:1 in LG22 to 2.50:1 in LG1 (Table 3). The largest differences in recombination rate between the female and male maps were observed in LG1, LG5, LG7, LG18, LG27 and LG29. Across all these linkage groups the female: male recombination ratios exceeded 2.0. LG22 was unusual in that: recombination rates were very similar between the sexes (i.e., 0.97:1). Within unique map positions, 504 SNPs were commonly shared between the two sexes, while significantly higher recombination rates we observed in majority of common locus intervals ($p < 0.01$) (Figure 6, Additional file 2).

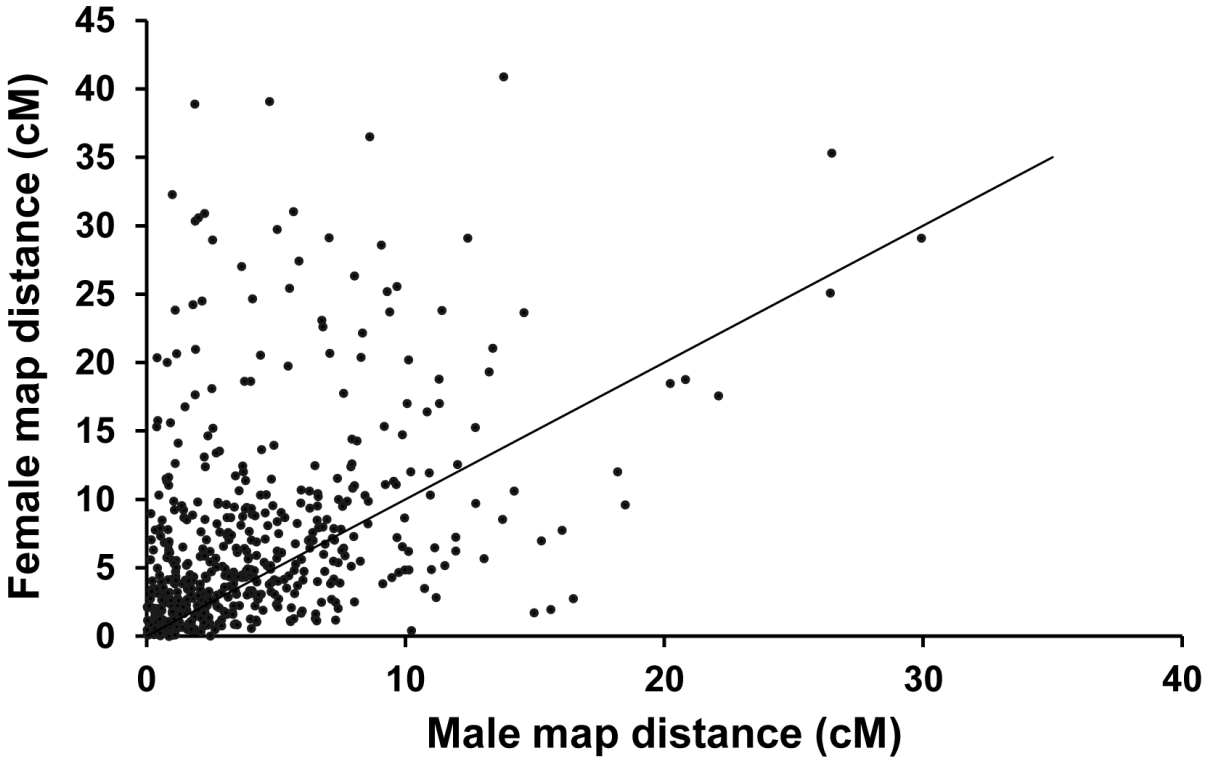

Figure 6 - Comparison of the recombination rate between female and male. The inter-marker distances (cM) for all pairs of adjacent markers from both female and male-specific maps were used. The diagonal line represents sex-equal recombination rates.

Integration and validation with physical map

The integration of the genetic map with the BAC-based physical map anchored 2,728 (83%) of the 3,307 physical map contigs (Table 5). Together with the 1,481 (44.8%) physical map contigs that were anchored previously (Ninwichian et al., 2012). we were able to anchor a total of 2,880 (87.1%) physical map contigs consisting of 28,416 BAC clones (92.9% of total BAC clones). The sizes of anchored physical map contigs varied from 66.0 kb to 2,005.8 kb (Additional file 2), with an average size of 301 kb. Together, a total of 867.4Mb of the physical map were integrated by genetic linkage map which accounted for about 90% of the channel catfish genome (Table 5). Detailed information regarding integration of linkage map and physical map is provided in Additional file 2.

The integration of linkage map and physical map enabled the cross-validation of the quality of the physical map and the genetic map (Table 6). A total of 1,467 physical map contigs containing 2,961 BES-associated SNPs were placed onto linkage maps. With 615 physical map contigs, two or more SNP markers were mapped that allowed the determination of orientation of the physical map contigs along the chromosome. With such contigs, the quality of physical map contigs was assessed based on the mapped markers. An illustration with linkage group 12 was provided in Figure 7. The vast majority of physical contigs were validated, but a small fraction of physical map contigs was found incorrectly assembly, or the ordering of the SNP markers onto the map was in error.

Table 5 - Integration of channel catfish linkage map with physical map.

Item	Number	Percentage
Number of physical map contigs*	3,307	100%
Number of physical map contigs with SNP markers	3,243	98.1%
Number of physical map contigs anchored to linkage map in this work	2,728	82.5%
Number of physical map contigs anchored in previous study#	1,481	44.8%
Total physical map contigs mapped to linkage map	2,880	87.1%
Total BAC clones in the catfish physical map*	30,582	100%
Total BAC clones mapped on the linkage map	28,416	92.9%
Total size of physical map contigs*	965,279	100%
Total size of anchored physical map contigs	867,364	89.9%

*Data obtained from Xu et al (Xu et al., 2007); #Data obtained from Ninwichian et al (Ninwichian et al., 2012)

Table 6 - Cross-validation between linkage map and physical map.

Item	Number
Number of physical map contigs with BES-associated SNPs	2,790
Number of physical map contigs anchored through BES-associated SNPs	1,467
Number of physical map contigs with at least two BES-associated SNPs	615
Number of physical map contigs mapped onto different LGs	47
Number of BAC clones with BES-associated SNPs	2,707
Number of BAC clones with at least two BES-associated SNPs	238
Number of BAC clones mapped onto different LGs	7

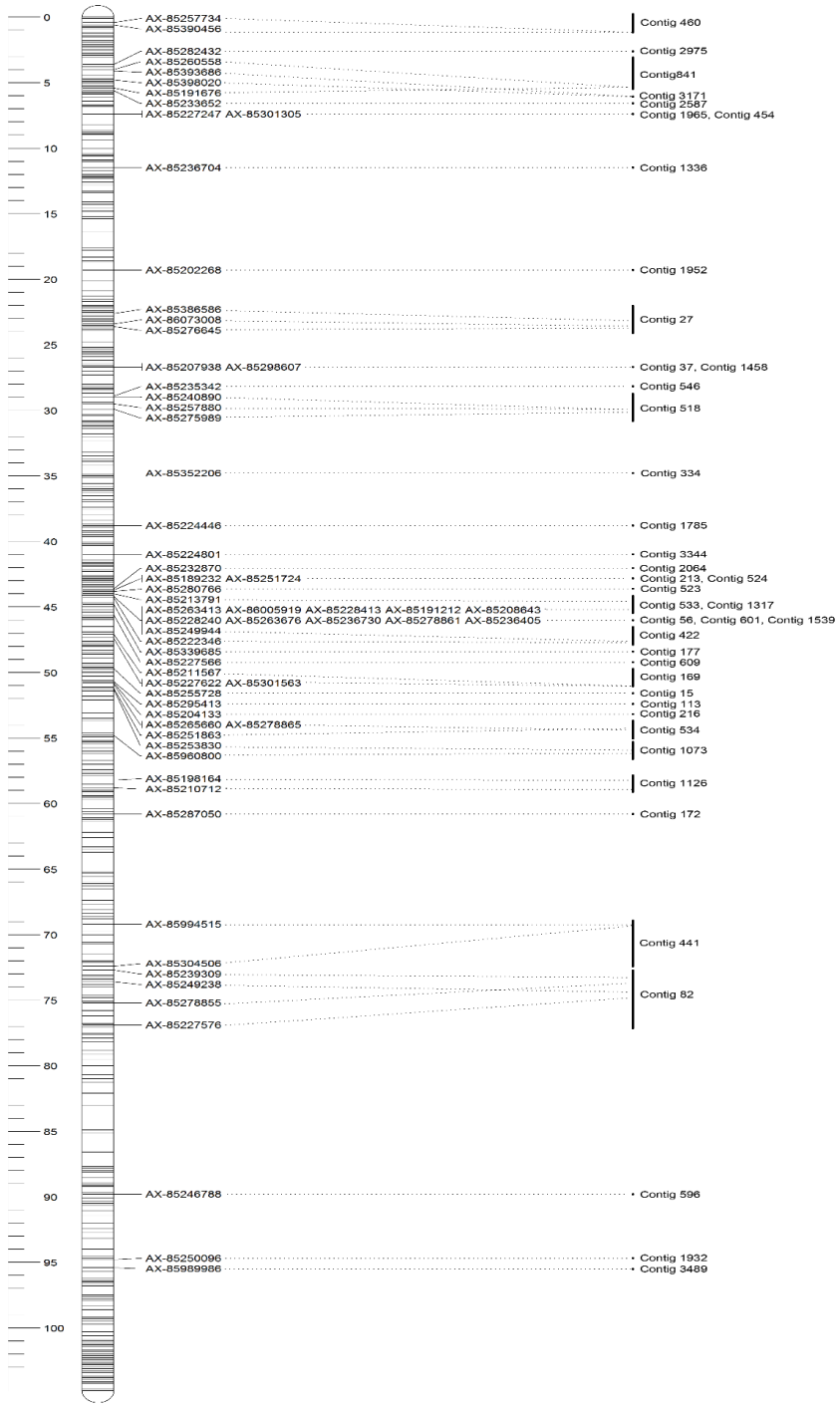

Figure 7- Illustration of integration of the linkage map (left) with the physical map (right). The linkage group 12 (LG12) was used for the illustration. Vertical bars represent physical map contigs containing at least two SNPs mapped onto the linkage map, and the dot spots indicate physical map contigs with only one SNP.

A total of 47 physical map contigs had markers that were mapped in different linkage groups, indicating the potential errors of the physical map assembly or the mapping errors of incorrectly assigned SNPs. These errors could be caused by SNPs falling into duplicated regions of genome. Moreover, of the 2,707 BAC clones with BES-associated SNPs, 238 BAC clones contained at least two BES-associated SNPs. Within this group, 7 BAC clones were mapped onto different LGs, suggesting the misplacement of those SNP markers onto the linkage groups. As an illustration, the integration of sex-averaged linkage map with physical map Contig72 and Contig534 were shown in Figure 8, presenting the correct and incorrect physical map assembly, respectively. The manual check of the potential assembly or mapping error warrants the correctness of both physical map and linkage map in the next step.

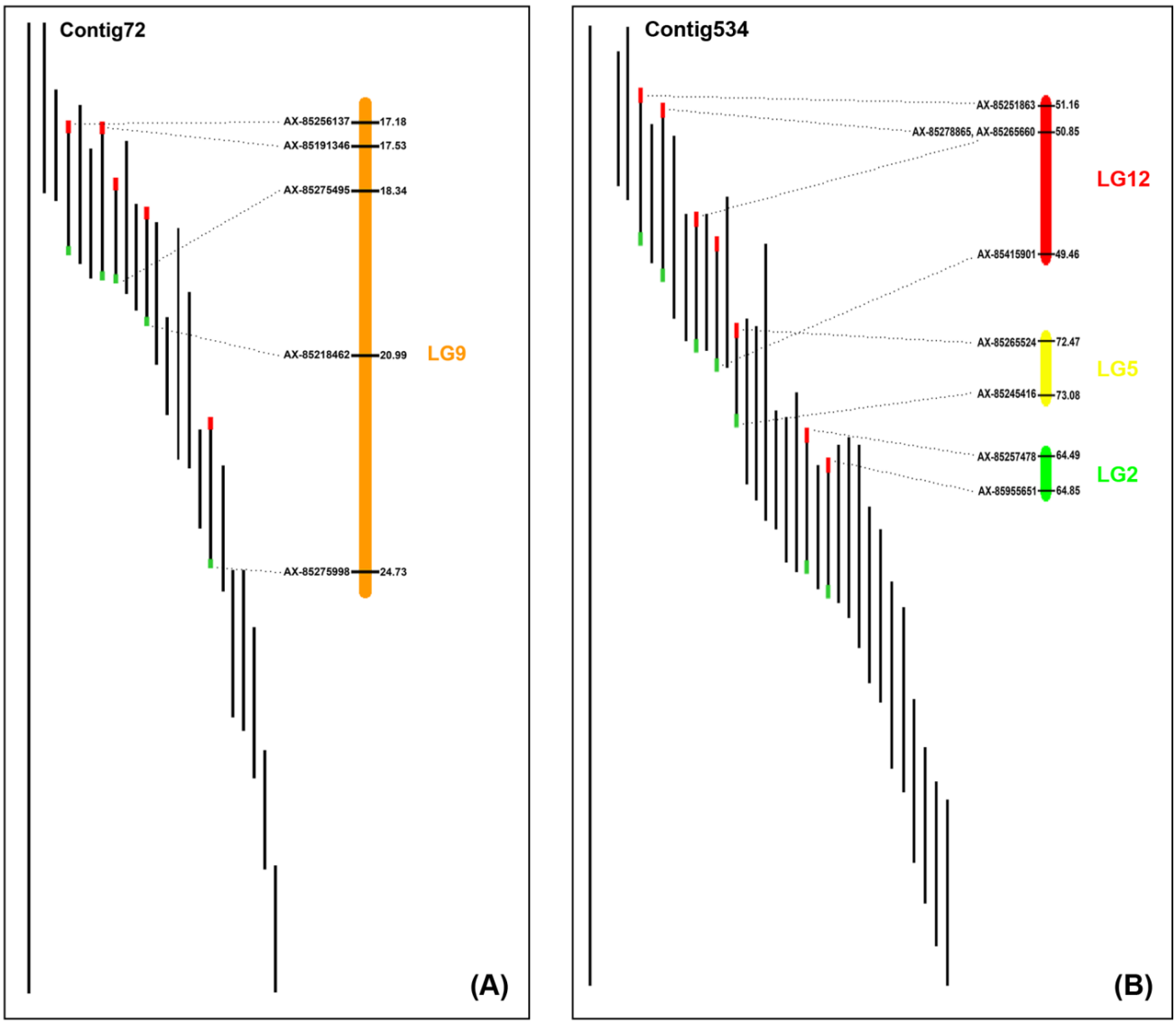

Figure 8 - Example of validation of physical map using the linkage map. (A) shows the correct physical map contig using Contig72 as an example; (B) shows the incorrect physical map contig using Contig534 as an example.

Physical distances were estimated based on position of SNP markers within each physical map contig, which allowed for estimation of the ratios of physical distance to genetic distance (Additional file 3). On the other hand, recombination frequencies can be calculated for physical

map contigs with multiple SNP markers mapped onto the linkage map. With the sex-average linkage map, the genetic size of 3,505.4 cM and the physical size of 965,279 kb based on the physical map, providing the average genetic size of 3.6 cM per Mb. The ratios observed from the 250 physical map contigs that contained multiple SNPs mapped onto the linkage map ranging from 0 cM to 2.26 cM. The markers with higher ratios might indicate the potential loci of recombination hot spots.

DISCUSSION

In the present work, we constructed a high-density genetic map for channel catfish. This map possesses the highest marker density among all the genetic linkage maps constructed for any aquaculture species. Taking advantage of the catfish 250K SNP array, we were able to efficiently and cost-effectively genotype 250,000 SNPs in the 576 fish from three mapping families (192 fish per family). Such a high-density linkage map should be valuable resource for analysis and fine-scale QTL mapping in catfish.

While the efficient SNP genotyping technology allowed the construction of high-density linkage map, the high-resolution was still not achieved. A large number of markers fell into ‘zero recombination clusters’ where no recombination events occur during meiosis between the markers among the fish used for mapping analysis. These represent closely arrayed adjacent SNP positions and their ordering is likely best achieved by assessing their order within the aligned physical map contigs. Cluster markers were mapped at the same position, however they add to the calculation efforts (Joinmap manual tutorial), and the genetic sizes were overestimated. In fact, the first version of our sex-average linkage map had genetic size at over 7,000 cM, which was double size of current genetic length. When “representative markers” (unique markers) were used, significant smaller genetic sizes were observed (Supplemental Figure 1). This phenomenon is common

happened in ultra-high density map building, which was considered be caused by presence of genotyping errors and missing data (Hackett and Broadfoot, 2003). In zebrafish, the genetic sizes of initial map were over 1,000 cM per chromosome. After removal of genotyping errors, the genetic sizes were reduced to around 100 cM (Howe et al., 2013). The genotype errors can also increase the proportion of incorrectly ordered maps, and this problem will be more severe as the distances between loci decreases. To reduce the effect of clustered markers on the map construction and reduce the computing load, we picked one representative anchor marker that had the most informative meiosis from each of these clusters in the linkage map construction. Afterwards, we rejoined the markers within the "zero recombination clusters" that were excluded during the initial mapping steps. This procedure relocated the informative markers onto the linkage maps based on the positions of their representative anchor marker. Such clustered markers are still valuable for the chromosome-scale scaffolding.

With the availability of such high-density mapped SNPs, the patterns of marker distribution across chromosomes can be examined. It appears that clustered markers were commonly found in regions around centromeres while less frequently found around the telomeres. This was consistent with observations in various genetic maps previously developed in fish species, such as tilapia (Kocher et al., 1998), medaka (Naruse et al., 2000), rainbow trout (Sakamoto et al., 2000), Atlantic salmon (Lorenz et al., 2010) and catfish (Liu et al., 2003; Ninwichian et al., 2012). One potential explanation is that the centromeres contain abundant tandemly repeated, heterochromatic DNA sequences (Choo, 1998). As shown in Figure 5, the distribution of linkage SNP markers cross chromosomes in channel catfish is consistent with the observation of telomere and centromere effects (Nachman and Churchill, 1996), which would result in a higher recombination rate near the telomeres while a lower recombination rate near the center of the chromosomes. The

recombination rates might be positively correlated with GC content, as in human (Coop and Przeworski, 2007a), pig (Tortereau et al., 2012), chicken (Groenen et al., 2009), rodent (Jensen-Seaman et al., 2004) and yeast (Petes, 2001), or correlated with some other genomic features such as gene density and the presence of genes determining recombination hotspots. The PRDM9 gene was recently found to determine the recombination hotspots in the mammalian genomes (Baudat et al., 2010; Myers et al., 2010; Parvanov et al., 2010). Future investigations on recombination landscape warrant the characterization of genomic features affecting the meiotic recombination in catfish upon the availability of fully-assembled genome sequences.

The suppression of recombination in males relative to the females observed in channel catfish (averaged female-to-male ratio is 1.7: 1) was consistent with our previous observation (Kucuktas et al., 2009) as well as many other studies. Recombination rates differ between the two sexes in many organisms where recombination occurs more frequently in the homogametic sex than in the heterogametic sex (Coop and Przeworski, 2007; Singer et al., 2002). The similar phenomenon was reported in many other fish species such as Atlantic salmon (1.38:1), rainbow trout (1.68:1), European sea bass (1.60:1), Arctic char (1.69:1) and silver carp (1.52:1) (Chistiakov et al., 2005; Guo et al., 2013; Lien et al., 2011; Rexroad et al., 2008; Singer et al., 2002a; Woram et al., 2004). Striking recombination differences between the sexes was observed in zebrafish (2.74:1) (Singer et al., 2002) and grass carp (2.0:1) (Xia et al., 2010). These observations indicated that even closely related fish species differ in genetic sizes and the extent of sexual dimorphism for recombination fraction (Coop and Przeworski, 2007) similarly as in mammals. Although the genetic basis for recombination bias between sexes remains unknown, several theories were proposed to explain this observation. One explanation from selection perspective suggests that selection pressure is stronger in male gametes than in female gametes during the haploid life stage. This difference

could lead to male specific selection to maintain beneficial haplotype to decrease the male recombination rate (Lenormand and Dutheil, 2005; Singer et al., 2002). An alternative explanation is that the female recombination rate is higher to compensate for the apparently less stringent checkpoint for achiasmatic chromosomes compared with males (Coop and Przeworski, 2007). In human, cytological studies suggested that sex specific differences in recombination may derive from chromatin differences established prior to the onset of the recombination pathway (Gruhn et al., 2013).

The high-density and the relatively high-resolution genetic map provide valuable resource for integrating the physical map and whole genome assemblies. In the present study, we anchored the catfish physical map to genetic linkage map through BES and physical map contig-specific sequences that contain SNP markers. With this linkage map of channel catfish, we were able to anchor 87% of the catfish BAC physical map contigs, covering approximately 92% of the catfish genome. This is a great improvement on map integration compared to our previous efforts that only anchored 44.8% of the catfish BAC physical map contigs accounting for 52.8% of the catfish genome. To our knowledge, this is also the highest percentage of physical maps integration with genetic maps that were obtained in any aquaculture species. The well-integrated map is useful for comprehensive comparative genomic analyses, fine-scale mapping of QTL and positional cloning for candidate genes (Palti et al., 2012). Moreover, the integrated map can be used as an important resource for the validation of the catfish whole genome assembly.

Conclusions

A high-density genetic linkage map was constructed in channel catfish, which provides a framework for validating and scaffolding the reference whole-genome sequences. With this map, we were able to integrate 87% physical map contigs which covered 92% of catfish genome. The

integrated map is a valuable resource for validating and improving the catfish whole genome assembly, and facilitates fine-scale QTL mapping and positional cloning of genes responsible for economically important traits. These resources will also be valuable for comparative genomic analysis with other teleost fish species.

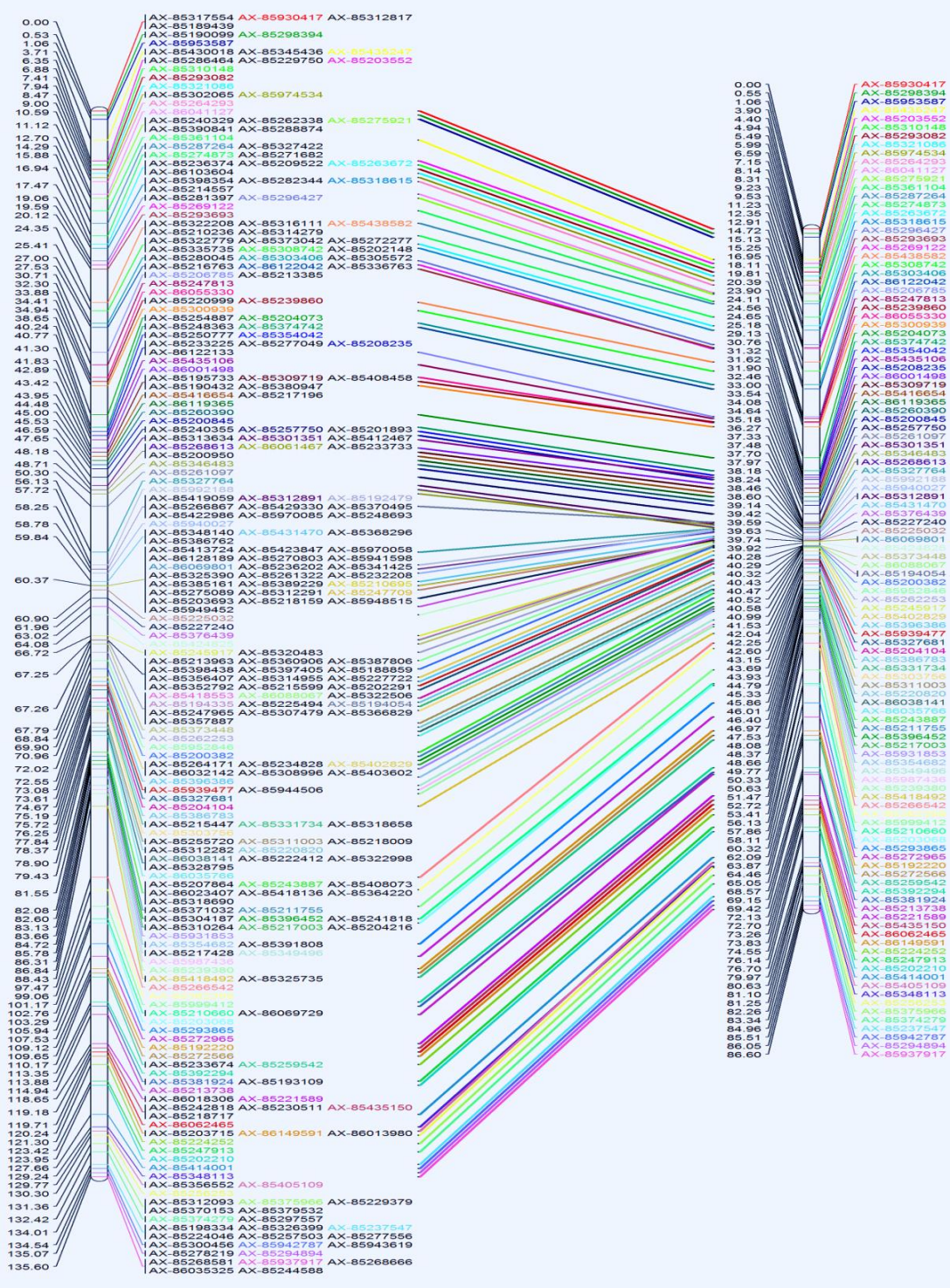

Supplemental Figure 1. Example of linkage map (LG4 of male map) constructed with all markers (left) and unique markers (right). Genetic size was overestimated due to the large number of clustered marker regions

References

Baudat, F., Buard, J., Grey, C., Fledel-Alon, A., Ober, C., Przeworski, M., Coop, G., de Massy, B., 2010. PRDM9 is a major determinant of meiotic recombination hotspots in humans and mice. Science 327, 836-840.

Cervera, M.T., Storme, V., Ivens, B., Gusmao, J., Liu, B.H., Hostyn, V., Van Slycken, J., Van Montagu, M., Boerjan, W., 2001. Dense genetic linkage maps of three Populus species (*Populus deltoides, P. nigra* and *P. trichocarpa*) based on AFLP and microsatellite markers. Genetics 158, 787-809.

Chistiakov, D.A., Hellemans, B., Haley, C.S., Law, A.S., Tsigenopoulos, C.S., Kotoulas, G., Bertotto, D., Libertini, A., Volckaert, F.A., 2005. A microsatellite linkage map of the European sea bass *Dicentrarchus labrax L*. Genetics 170, 1821-1826.

Choo, K.H.A., 1998. Why is the centromere so cold? Genome research 8, 81-82.

Coop, G., Przeworski, M., 2007. An evolutionary view of human recombination. Nature reviews Genetics 8, 23-34.

Garcia-Dorado, A., Gallego, A., 1992. On the use of the classical tests for detecting linkage. Journal of heredity 83, 143-146.

Groenen, M.A., Wahlberg, P., Foglio, M., Cheng, H.H., Megens, H.J., Crooijmans, R.P., Besnier, F., Lathrop, M., Muir, W.M., Wong, G.K., Gut, I., Andersson, L., 2009. A high-density SNP-based linkage map of the chicken genome reveals sequence features correlated with recombination rate. Genome research 19, 510-519.

Gruhn, J.R., Rubio, C., Broman, K.W., Hunt, P.A., Hassold, T., 2013. Cytological studies of human meiosis: sex-specific differences in recombination originate at, or prior to, establishment of double-strand breaks. PloS one 8, e85075.

Guo, W.J., Tong, J.G., Yu, X.M., Zhu, C.K., Feng, X., Fu, B.D., He, S.P., Zeng, F.Z., Wang, X.H., Liu, H.Y., Liu, L.S., 2013. A second generation genetic linkage map for silver carp (*Hypophthalmichehys molitrix*) using microsatellite markers. Aquaculture 412, 97-106.

Hackett, C.A., Broadfoot, L.B., 2003. Effects of genotyping errors, missing values and segregation distortion in molecular marker data on the construction of linkage maps. Heredity 90, 33-38.

Haldane, J., 1919. The combination of linkage values, and the calculation of distances between the loci of linked factors. J Genet 8 (29), 299-309.

Howe, K., Clark, M.D., Torroja, C.F., Torrance, J., Berthelot, C., Muffato, M., Collins, J.E., Humphray, S., McLaren, K., Matthews, L., McLaren, S., Sealy, I., Caccamo, M., Churcher, C., Scott, C., Barrett, J.C., Koch, R., Rauch, G.J., White, S., Chow, W., Kilian, B., Quintais, L.T., Guerra-Assuncao, J.A., Zhou, Y., Gu, Y., Yen, J., Vogel, J.H., Eyre, T., Redmond, S., Banerjee, R., Chi, J., Fu, B., Langley, E., Maguire, S.F., Laird, G.K., Lloyd, D., Kenyon, E., Donaldson, S., Sehra, H., Almeida-King, J., Loveland, J., Trevanion, S., Jones, M., Quail, M., Willey, D., Hunt, A., Burton, J., Sims, S., McLay, K., Plumb, B., Davis, J., Clee, C., Oliver, K., Clark, R., Riddle, C., Elliot, D., Threadgold, G., Harden, G., Ware, D., Mortimore, B., Kerry, G., Heath, P., Phillimore, B., Tracey, A., Corby, N., Dunn, M., Johnson, C., Wood, J., Clark, S., Pelan, S., Griffiths, G., Smith, M., Glithero, R., Howden, P., Barker, N., Stevens, C., Harley, J., Holt, K., Panagiotidis, G., Lovell, J., Beasley, H., Henderson, C., Gordon, D., Auger, K., Wright, D., Collins, J., Raisen, C., Dyer, L., Leung, K., Robertson, L., Ambridge, K., Leongamornlert, D., McGuire, S., Gilderthorp, R., Griffiths, C., Manthravadi, D., Nichol, S., Barker, G., Whitehead, S., Kay, M., Brown, J., Murnane, C., Gray, E., Humphries, M., Sycamore, N., Barker, D., Saunders, D., Wallis, J., Babbage, A., Hammond, S., Mashreghi-Mohammadi, M., Barr, L., Martin, S., Wray, P., Ellington, A., Matthews, N., Ellwood, M.,

Woodmansey, R., Clark, G., Cooper, J., Tromans, A., Grafham, D., Skuce, C., Pandian, R., Andrews, R., Harrison, E., Kimberley, A., Garnett, J., Fosker, N., Hall, R., Garner, P., Kelly, D., Bird, C., Palmer, S., Gehring, I., Berger, A., Dooley, C.M., Ersan-Urun, Z., Eser, C., Geiger, H., Geisler, M., Karotki, L., Kirn, A., Konantz, J., Konantz, M., Oberlander, M., Rudolph-Geiger, S., Teucke, M., Osoegawa, K., Zhu, B., Rapp, A., Widaa, S., Langford, C., Yang, F., Carter, N.P., Harrow, J., Ning, Z., Herrero, J., Searle, S.M., Enright, A., Geisler, R., Plasterk, R.H., Lee, C., Westerfield, M., de Jong, P.J., Zon, L.I., Postlethwait, J.H., Nusslein-Volhard, C., Hubbard, T.J., Roest Crollius, H., Rogers, J., Stemple, D.L., Begum, S., Lloyd, C., Lanz, C., Raddatz, G., Schuster, S.C., 2013. The zebrafish reference genome sequence and its relationship to the human genome. Nature 496, 498-503.

Jensen-Seaman, M.I., Furey, T.S., Payseur, B.A., Lu, Y., Roskin, K.M., Chen, C.F., Thomas, M.A., Haussler, D., Jacob, H.J., 2004. Comparative recombination rates in the rat, mouse, and human genomes. Genome research 14, 528-538.

Jiang, Y., Ninwichian, P., Liu, S., Zhang, J., Kucuktas, H., Sun, F., Kaltenboeck, L., Sun, L., Bao, L., Liu, Z., 2013. Generation of physical map contig-specific sequences useful for whole genome sequence scaffolding. PloS one 8, e78872.

Kinghorn, B., van der Werf, J., 2000. Identifying and incorporating genetic markers and major genes in animal breeding programs. Curso desarrollado en Belo Horizonte 31.

Kocher, T.D., Lee, W.J., Sobolewska, H., Penman, D., McAndrew, B., 1998. A genetic linkage map of a cichlid fish, the tilapia (*Oreochromis niloticus*). Genetics 148, 1225-1232.

Kosambi, D., 1943. The estimation of map distances from recombination values. Annals of Eugenics 12, 172-175.

Kucuktas, H., Wang, S., Li, P., He, C., Xu, P., Sha, Z., Liu, H., Jiang, Y., Baoprasertkul, P.,

Somridhivej, B., Wang, Y., Abernathy, J., Guo, X., Liu, L., Muir, W., Liu, Z., 2009. Construction of genetic linkage maps and comparative genome analysis of catfish using gene-associated markers. Genetics 181, 1649-1660.

Lenormand, T., Dutheil, J., 2005. Recombination difference between sexes: a role for haploid selection. PLoS biology 3, e63.

Lien, S., Gidskehaug, L., Moen, T., Hayes, B.J., Berg, P.R., Davidson, W.S., Omholt, S.W., Kent, M.P., 2011. A dense SNP-based linkage map for Atlantic salmon (*Salmo salar*) reveals extended chromosome homeologies and striking differences in sex-specific recombination patterns. BMC genomics 12, 615.

Liu, H., Jiang, Y.L., Wang, S.L., Ninwichian, P., Somridhivej, B., Xu, P., Abernathy, J., Kucuktas, H., Liu, Z.J., 2009. Comparative analysis of catfish BAC end sequences with the zebrafish genome. BMC genomics 10, 592.

Liu, S., Sun, L., Li, Y., Sun, F., Jiang, Y., Zhang, Y., Zhang, J., Feng, J., Kaltenboeck, L., Kucuktas, H., Liu, Z., 2014. Development of the catfish 250K SNP array for genome-wide association studies. BMC research notes 7, 135.

Lorenz, S., Brenna-Hansen, S., Moen, T., Roseth, A., Davidson, W.S., Omholt, S.W., Lien, S., 2010. BAC-based upgrading and physical integration of a genetic SNP map in Atlantic salmon. Animal genetics 41, 48-54.

Myers, S., Bowden, R., Tumian, A., Bontrop, R.E., Freeman, C., MacFie, T.S., McVean, G., Donnelly, P., 2010. Drive against hotspot motifs in primates implicates the PRDM9 gene in meiotic recombination. Science 327, 876-879.

Nachman, M.W., Churchill, G.A., 1996. Heterogeneity in rates of recombination across the mouse genome. Genetics 142, 537-548.

Naruse, K., Fukamachi, S., Mitani, H., Kondo, M., Matsuoka, T., Kondo, S., Hanamura, N., Morita, Y., Hasegawa, K., Nishigaki, R., Shimada, A., Wada, H., Kusakabe, T., Suzuki, N., Kinoshita, M., Kanamori, A., Terado, T., Kimura, H., Nonaka, M., Shima, A., 2000. A detailed linkage map of medaka, *Oryzias latipes*: comparative genomics and genome evolution. Genetics 154, 1773-1784.

Ninwichian, P., Peatman, E., Liu, H., Kucuktas, H., Somridhivej, B., Liu, S., Li, P., Jiang, Y., Sha, Z., Kaltenboeck, L., Abernathy, J.W., Wang, W., Chen, F., Lee, Y., Wong, L., Wang, S., Lu, J., Liu, Z., 2012. Second-generation genetic linkage map of catfish and its integration with the BAC-based physical map. G3:Genes| Genomes| Genetics 2, 1233-1241.

Ott, J., 1999. Analysis of human genetic linkage. JHU Press.

Palti, Y., Genet, C., Gao, G., Hu, Y., You, F.M., Boussaha, M., Rexroad, C.E., Luo, M.C., 2012. A second generation integrated map of the rainbow trout (*Oncorhynchus mykiss*) genome: analysis of conserved synteny with model fish genomes. Marine biotechnology 14, 343-357.

Parvanov, E.D., Petkov, P.M., Paigen, K., 2010. Prdm9 controls activation of mammalian recombination hotspots. Science 327, 835.

Petes, T.D., 2001. Meiotic recombination hot spots and cold spots. Nature reviews. Genetics 2, 360-369.

Recknagel, H., Elmer, K.R., Meyer, A., 2013. A hybrid genetic linkage map of two ecologically and morphologically divergent Midas cichlid fishes (*Amphilophus spp*.) obtained by massively parallel DNA sequencing (ddRADSeq). G3: Genes| Genomes| Genetics 3, 65-74.

Rexroad, C.E., 3rd, Palti, Y., Gahr, S.A., Vallejo, R.L., 2008. A second generation genetic map for rainbow trout (*Oncorhynchus mykiss*). BMC genetics 9, 74.

Sakamoto, T., Danzmann, R.G., Gharbi, K., Howard, P., Ozaki, A., Khoo, S.K., Woram, R.A.,

Okamoto, N., Ferguson, M.M., Holm, L.E., Guyomard, R., Hoyheim, B., 2000. A microsatellite linkage map of rainbow trout (*Oncorhynchus mykiss*) characterized by large sex-specific differences in recombination rates. Genetics 155, 1331-1345.

Singer, A., Perlman, H., Yan, Y., Walker, C., Corley-Smith, G., Brandhorst, B., Postlethwait, J., 2002. Sex-specific recombination rates in zebrafish (*Danio rerio*). Genetics 160, 649-657.

Stam, P., 1993. Construction of integrated genetic linkage maps by means of a new computer package: Join Map. The plant journal 3, 739-744.

Tortereau, F., Servin, B., Frantz, L., Megens, H.J., Milan, D., Rohrer, G., Wiedmann, R., Beever, J., Archibald, A.L., Schook, L.B., Groenen, M.A., 2012. A high density recombination map of the pig reveals a correlation between sex-specific recombination and GC content. BMC genomics 13, 586.

Van Ooijen, J., 2006. JoinMap 4. Software for the calculation of genetic linkage maps in experimental populations. Kyazma BV, Wageningen, Netherlands.

Voorrips, R., 2002. MapChart: software for the graphical presentation of linkage maps and QTLs. Journal of heredity 93, 77-78.

Waldbieser, G.C., Bosworth, B.G., Nonneman, D.J., Wolters, W.R., 2001. A microsatellite-based genetic linkage map for channel catfish, *Ictalurus punctatus*. Genetics 158, 727-734.

Woram, R.A., McGowan, C., Stout, J.A., Gharbi, K., Ferguson, M.M., Hoyheim, B., Davidson, E.A., Davidson, W.S., Rexroad, C., Danzmann, R.G., 2004. A genetic linkage map for Arctic char (*Salvelinus alpinus*): evidence for higher recombination rates and segregation distortion in hybrid versus pure strain mapping parents. Genome 47 (2), 304-315.

Wu, Y., Close, T.J., Lonardi, S., 2011. Accurate construction of consensus genetic maps via integer linear programming. IEEE/ACM Transactions on computational biology and bioinformatics

8, 381-394.

Xia, J.H., Liu, F., Zhu, Z.Y., Fu, J., Feng, J., Li, J., Yue, G.H., 2010. A consensus linkage map of the grass carp (*Ctenopharyngodon idella*) based on microsatellites and SNPs. BMC genomics 11, 135.

Xu, P., Wang, S., Liu, L., Peatman, E., Somridhivej, B., Thimmapuram, J., Gong, G., Liu, Z., 2006. Channel catfish BAC-end sequences for marker development and assessment of syntenic conservation with other fish species. Animal genetics 37, 321-326.

Xu, P., Wang, S.L., Liu, L., Thorsen, J., Kucuktas, H., Liu, Z.J., 2007. A BAC-based physical map of the channel catfish genome. Genomics 90, 380-388.

Table S1 (1): Example (LG1) of detailed information of sex-average linkage map

LGs	MarkerID	Map position(cM)
LG1	AX-85238541	0
LG1	AX-85375738	0
LG1	AX-85410631	0
LG1	AX-85410374	0.5
LG1	AX-85237828	0.61
LG1	AX-85275059	0.61
LG1	AX-85437510	5.01
LG1	AX-85308625	6.09
LG1	AX-85330376	6.09
LG1	AX-85316136	6.82
LG1	AX-85293889	6.92
LG1	AX-85359715	7.11
LG1	AX-85323305	7.22
LG1	AX-85272198	7.4
LG1	AX-86097766	7.89
LG1	AX-85281635	8.21
LG1	AX-85295991	9.03
LG1	AX-85310229	9.03
LG1	AX-85383123	9.03
LG1	AX-85228614	9.26
LG1	AX-85204340	10.33
LG1	AX-85254174	10.62
LG1	AX-85341083	11.51
LG1	AX-85210269	13.24
LG1	AX-85303782	13.24
LG1	AX-85947692	13.7
LG1	AX-85428816	17.21
LG1	AX-85300238	18.24
LG1	AX-85280640	18.31
LG1	AX-85315730	19.06
LG1	AX-85395535	20.63
LG1	AX-85357756	20.65
LG1	AX-85220640	21.4
LG1	AX-85241609	21.53
LG1	AX-86008417	21.81
LG1	AX-85225921	21.83
LG1	AX-85245154	21.83
LG1	AX-85230705	22.09
LG1	AX-85272770	22.09
LG1	AX-86043118	22.09
LG1	AX-85224792	22.32
LG1	AX-85363395	22.32
LG1	AX-85339733	22.59
LG1	AX-85264710	22.61
LG1	AX-85275274	22.61
LG1	AX-85306500	22.61
LG1	AX-85337349	22.61

LG1	AX-85333231	23.09
LG1	AX-86023282	23.09
LG1	AX-85341950	23.13
LG1	AX-85975520	23.13
LG1	AX-85370762	23.7
LG1	AX-85406120	23.7
LG1	AX-85233724	25.71
LG1	AX-85284152	26.83
LG1	AX-85366231	26.83
LG1	AX-85300351	27.23
LG1	AX-85932706	27.4
LG1	AX-85276603	27.79
LG1	AX-85330725	27.79
LG1	AX-85366155	27.79
LG1	AX-85399862	27.79
LG1	AX-85406230	27.79
LG1	AX-85443918	27.79
LG1	AX-85423952	28.21
LG1	AX-85299829	28.48
LG1	AX-85401341	28.48
LG1	AX-86016858	28.48
LG1	AX-85201571	29.36
LG1	AX-85262604	30.21
LG1	AX-85361455	31.04
LG1	AX-85440933	31.46
LG1	AX-85294682	31.55
LG1	AX-85205423	31.59
LG1	AX-85196610	31.8
LG1	AX-85269277	31.8
LG1	AX-85282901	31.8
LG1	AX-85345692	31.8
LG1	AX-85193389	31.89
LG1	AX-85378064	32.41
LG1	AX-85391113	33.2
LG1	AX-85345084	33.95
LG1	AX-85249569	34.25
LG1	AX-85353124	34.81
LG1	AX-85425672	34.81
LG1	AX-85406101	35.06
LG1	AX-86038570	35.06
LG1	AX-85947435	35.93
LG1	AX-86121832	36.06
LG1	AX-85228787	36.88
LG1	AX-85306522	36.88
LG1	AX-85420849	36.88
LG1	AX-86006423	36.88
LG1	AX-86118426	36.88
LG1	AX-85331723	37.36
LG1	AX-85379296	37.62
LG1	AX-86137223	38.55

LG1	AX-85424458	39.03
LG1	AX-85965649	39.03
LG1	AX-85294918	39.15
LG1	AX-85198901	39.18
LG1	AX-85214962	39.47
LG1	AX-85378643	39.47
LG1	AX-85301559	39.64
LG1	AX-85283878	39.68
LG1	AX-86017118	39.78
LG1	AX-85207103	39.81
LG1	AX-85229579	39.81
LG1	AX-85273486	39.81
LG1	AX-85324297	39.81
LG1	AX-85347502	39.81
LG1	AX-85381801	39.81
LG1	AX-85397632	39.81
LG1	AX-85429292	39.81
LG1	AX-85442014	39.81
LG1	AX-85924574	39.81
LG1	AX-85256775	40.05
LG1	AX-85367338	40.05
LG1	AX-85417800	40.05
LG1	AX-85250846	40.25
LG1	AX-85202024	40.3
LG1	AX-85243152	40.3
LG1	AX-85361959	40.3
LG1	AX-85371231	40.3
LG1	AX-85364127	40.6
LG1	AX-85192137	40.62
LG1	AX-85279948	40.62
LG1	AX-85313507	40.62
LG1	AX-85347655	40.62
LG1	AX-85373973	40.62
LG1	AX-86131818	40.62
LG1	AX-85242802	40.71
LG1	AX-85280413	40.71
LG1	AX-85366409	40.71
LG1	AX-85237991	41.19
LG1	AX-85206069	41.63
LG1	AX-86076106	41.63
LG1	AX-86146398	41.63
LG1	AX-86057397	42.35
LG1	AX-85230200	42.58
LG1	AX-85282177	42.58
LG1	AX-85309830	42.58
LG1	AX-85369354	42.58
LG1	AX-85950566	42.66
LG1	AX-85221299	42.72
LG1	AX-85196598	42.96
LG1	AX-85261076	43.21

LG1	AX-85255388	43.25
LG1	AX-85980759	43.41
LG1	AX-85206949	43.98
LG1	AX-85315674	43.98
LG1	AX-85383122	43.98
LG1	AX-86078397	43.98
LG1	AX-86113115	44.06
LG1	AX-85402111	44.09
LG1	AX-85229139	44.23
LG1	AX-85355081	44.58
LG1	AX-85198606	45.8
LG1	AX-85190418	46.58
LG1	AX-85309208	47.08
LG1	AX-85199970	47.15
LG1	AX-85246672	47.62
LG1	AX-85409074	47.77
LG1	AX-86043743	48.08
LG1	AX-85351038	48.62
LG1	AX-85318964	48.64
LG1	AX-85430811	48.9
LG1	AX-85231605	49.18
LG1	AX-85415805	49.23
LG1	AX-86010557	49.34
LG1	AX-85269210	49.77
LG1	AX-85354916	49.77
LG1	AX-85385959	49.78
LG1	AX-85308423	50.15
LG1	AX-85314920	50.65
LG1	AX-85329636	50.65
LG1	AX-85272981	52.36
LG1	AX-85342237	52.36
LG1	AX-85414871	52.36
LG1	AX-85342241	53.64
LG1	AX-85924567	54.34
LG1	AX-85337888	54.55
LG1	AX-85257878	54.81
LG1	AX-85283695	55.29
LG1	AX-85328744	55.58
LG1	AX-85349891	55.78
LG1	AX-85306609	55.81
LG1	AX-85386614	55.98
LG1	AX-86030917	55.98
LG1	AX-85233010	56.11
LG1	AX-85276750	56.15
LG1	AX-85214584	57.55
LG1	AX-85312351	58.16
LG1	AX-85319113	58.5
LG1	AX-85206927	58.65
LG1	AX-85228203	58.77
LG1	AX-85211876	59.04

LG1	AX-85246380	59.07
LG1	AX-85313094	59.07
LG1	AX-86108414	59.11
LG1	AX-85200812	59.26
LG1	AX-85227777	59.26
LG1	AX-85274080	59.26
LG1	AX-85360928	59.26
LG1	AX-85246458	59.27
LG1	AX-85415640	59.27
LG1	AX-85230523	59.34
LG1	AX-85272551	59.34
LG1	AX-85289156	59.34
LG1	AX-85321554	59.34
LG1	AX-85336873	59.34
LG1	AX-85344885	59.34
LG1	AX-85365068	59.34
LG1	AX-85411680	59.34
LG1	AX-85417363	59.34
LG1	AX-86034645	59.35
LG1	AX-85372551	59.37
LG1	AX-85438706	59.43
LG1	AX-85220600	59.64
LG1	AX-85285881	59.64
LG1	AX-85348142	59.69
LG1	AX-85239163	59.75
LG1	AX-85245836	59.82
LG1	AX-85349601	59.82
LG1	AX-85980096	59.82
LG1	AX-86006093	59.82
LG1	AX-85932856	60.03
LG1	AX-85426956	60.16
LG1	AX-86026712	60.16
LG1	AX-85426980	60.18
LG1	AX-85344775	60.36
LG1	AX-85403795	60.44
LG1	AX-85985651	60.56
LG1	AX-85394312	60.59
LG1	AX-85205981	60.67
LG1	AX-85399633	60.67
LG1	AX-85407472	60.67
LG1	AX-85427327	60.67
LG1	AX-85440392	60.91
LG1	AX-85428738	61.05
LG1	AX-85431377	61.38
LG1	AX-85234816	61.54
LG1	AX-85260288	61.54
LG1	AX-85282197	61.54
LG1	AX-85285849	61.54
LG1	AX-85395344	61.54
LG1	AX-85188724	61.6

LG1 AX-85270622 61.6
LG1 AX-85332733 61.6
LG1 AX-85994860 61.6
LG1 AX-85219738 61.61
LG1 AX-85223895 61.61
LG1 AX-85357652 61.61
LG1 AX-85401835 61.61
LG1 AX-85263292 61.63
LG1 AX-85219924 61.72
LG1 AX-85376347 61.82
LG1 AX-85190244 61.87
LG1 AX-85306395 61.87
LG1 AX-85315436 61.87
LG1 AX-85349574 62.1
LG1 AX-85287992 62.21
LG1 AX-85409799 62.21
LG1 AX-85252775 62.29
LG1 AX-85203437 62.31
LG1 AX-85207042 62.31
LG1 AX-85213436 62.31
LG1 AX-85228574 62.31
LG1 AX-85310570 62.31
LG1 AX-85338450 62.31
LG1 AX-85419616 62.31
LG1 AX-85209400 62.55
LG1 AX-85438168 62.66
LG1 AX-85193606 62.75
LG1 AX-85333982 62.75
LG1 AX-85374913 62.75
LG1 AX-85196411 62.81
LG1 AX-85221041 62.92
LG1 AX-85247360 62.92
LG1 AX-85295245 62.92
LG1 AX-85349176 62.92
LG1 AX-85225406 63.03
LG1 AX-85383415 63.03
LG1 AX-85407186 63.03
LG1 AX-86004019 63.03
LG1 AX-86056502 63.03
LG1 AX-85295005 63.11
LG1 AX-85423395 63.34
LG1 AX-85442624 63.34
LG1 AX-85206995 63.39
LG1 AX-85236244 63.39
LG1 AX-85278402 63.39
LG1 AX-85383657 63.39
LG1 AX-85342599 63.56
LG1 AX-85404700 63.67
LG1 AX-85344758 63.76
LG1 AX-85397413 63.76

LG1	AX-85371678	64.03
LG1	AX-85352536	64.1
LG1	AX-85400377	64.1
LG1	AX-85322952	64.24
LG1	AX-85190291	64.31
LG1	AX-85245866	64.31
LG1	AX-85376403	64.31
LG1	AX-85923003	64.31
LG1	AX-85394243	64.45
LG1	AX-85364327	64.49
LG1	AX-85339605	64.57
LG1	AX-85384959	64.57
LG1	AX-85409410	64.57
LG1	AX-85252566	64.59
LG1	AX-85284145	64.59
LG1	AX-85303362	64.59
LG1	AX-85430515	64.59
LG1	AX-85437597	64.59
LG1	AX-85235681	64.67
LG1	AX-85337919	64.74
LG1	AX-85232087	65.12
LG1	AX-85297871	65.12
LG1	AX-85341131	65.12
LG1	AX-85372796	65.12
LG1	AX-85411424	65.12
LG1	AX-85424226	65.12
LG1	AX-85424486	65.12
LG1	AX-85315472	65.18
LG1	AX-85319413	65.18
LG1	AX-85343044	65.18
LG1	AX-85200246	65.3
LG1	AX-85305897	65.3
LG1	AX-85365072	65.3
LG1	AX-85416224	65.3
LG1	AX-85196152	65.34
LG1	AX-85429418	65.34
LG1	AX-85430661	65.34
LG1	AX-85373049	65.35
LG1	AX-86151395	65.48
LG1	AX-85353204	65.68
LG1	AX-85285879	65.69
LG1	AX-85381369	65.69
LG1	AX-85406844	65.69
LG1	AX-85411760	65.69
LG1	AX-85432593	65.69
LG1	AX-86041679	65.69
LG1	AX-85304368	65.77
LG1	AX-85307713	65.77
LG1	AX-85345295	65.77
LG1	AX-85356070	65.77

LG1	AX-85359383	65.77
LG1	AX-85394415	65.77
LG1	AX-85419288	65.77
LG1	AX-85275718	65.89
LG1	AX-85194345	66.21
LG1	AX-85405335	66.21
LG1	AX-85932792	66.21
LG1	AX-85966307	66.32
LG1	AX-85211166	66.39
LG1	AX-85344295	66.39
LG1	AX-85372546	66.39
LG1	AX-85419285	66.39
LG1	AX-85422833	66.39
LG1	AX-86138392	66.39
LG1	AX-85929962	66.65
LG1	AX-85350173	66.67
LG1	AX-85407023	66.67
LG1	AX-85401212	66.72
LG1	AX-85199446	66.79
LG1	AX-85254855	66.79
LG1	AX-85352296	66.79
LG1	AX-85399311	66.79
LG1	AX-85412052	66.79
LG1	AX-85442597	66.81
LG1	AX-85441332	66.97
LG1	AX-85263418	67.07
LG1	AX-85429572	67.07
LG1	AX-85441602	67.07
LG1	AX-86159151	67.07
LG1	AX-85296393	67.1
LG1	AX-85367835	67.13
LG1	AX-85415997	67.17
LG1	AX-85398350	67.21
LG1	AX-85253486	67.31
LG1	AX-85407007	67.31
LG1	AX-85425665	67.31
LG1	AX-85220435	67.46
LG1	AX-85373776	67.48
LG1	AX-85387819	67.48
LG1	AX-85196287	67.54
LG1	AX-85330489	67.56
LG1	AX-85200170	67.61
LG1	AX-85218851	67.61
LG1	AX-85239106	67.61
LG1	AX-85287017	67.61
LG1	AX-85309900	67.61
LG1	AX-85432780	67.61
LG1	AX-85991818	67.61
LG1	AX-85235325	67.74
LG1	AX-85249695	67.74

LG1	AX-85292343	67.74
LG1	AX-85329022	67.74
LG1	AX-85388774	67.74
LG1	AX-85393167	67.74
LG1	AX-86091484	67.74
LG1	AX-86136422	67.74
LG1	AX-85386948	67.76
LG1	AX-86042375	67.76
LG1	AX-85283638	67.81
LG1	AX-85190734	67.86
LG1	AX-85194886	67.86
LG1	AX-85204198	67.86
LG1	AX-85217073	67.86
LG1	AX-85270219	67.86
LG1	AX-85284669	67.86
LG1	AX-85374483	67.86
LG1	AX-85394576	67.86
LG1	AX-85396011	67.86
LG1	AX-86098934	67.86
LG1	AX-86106270	67.86
LG1	AX-86124748	67.86
LG1	AX-85234163	67.9
LG1	AX-85255192	67.9
LG1	AX-85304081	67.9
LG1	AX-85357042	67.9
LG1	AX-85416101	67.9
LG1	AX-86084168	67.9
LG1	AX-85218788	68.12
LG1	AX-85273248	68.12
LG1	AX-85315052	68.12
LG1	AX-86159953	68.12
LG1	AX-85344978	68.14
LG1	AX-85199230	68.18
LG1	AX-85233379	68.18
LG1	AX-85281032	68.18
LG1	AX-85326783	68.18
LG1	AX-85378838	68.18
LG1	AX-85402537	68.18
LG1	AX-85412388	68.18
LG1	AX-85211041	68.29
LG1	AX-85276260	68.29
LG1	AX-85311691	68.29
LG1	AX-85333847	68.29
LG1	AX-85335438	68.29
LG1	AX-86118547	68.29
LG1	AX-85423670	68.4
LG1	AX-85342564	68.45
LG1	AX-85275193	68.47
LG1	AX-85324000	68.47
LG1	AX-85339264	68.47

LG1	AX-85419762	68.47
LG1	AX-85956450	68.47
LG1	AX-85274785	68.61
LG1	AX-85207135	68.65
LG1	AX-85311111	68.65
LG1	AX-85391836	68.65
LG1	AX-85436941	68.65
LG1	AX-85969276	68.65
LG1	AX-85415680	68.67
LG1	AX-85207421	68.69
LG1	AX-85417416	68.69
LG1	AX-85367163	68.77
LG1	AX-85398669	68.83
LG1	AX-85926824	68.83
LG1	AX-85235176	68.86
LG1	AX-85232755	68.94
LG1	AX-85243010	68.94
LG1	AX-85304590	68.94
LG1	AX-85346170	68.94
LG1	AX-85382821	68.94
LG1	AX-85401343	68.94
LG1	AX-85403898	68.94
LG1	AX-85430257	68.94
LG1	AX-85984573	68.97
LG1	AX-85199649	68.99
LG1	AX-85214414	68.99
LG1	AX-85268275	69.01
LG1	AX-85365079	69.01
LG1	AX-85371025	69.01
LG1	AX-85436660	69.01
LG1	AX-85260718	69.05
LG1	AX-85924487	69.05
LG1	AX-85927107	69.05
LG1	AX-85208011	69.08
LG1	AX-85212557	69.08
LG1	AX-85320187	69.17
LG1	AX-85331615	69.26
LG1	AX-85401199	69.26
LG1	AX-85438296	69.26
LG1	AX-85216375	69.29
LG1	AX-85239437	69.29
LG1	AX-85369430	69.29
LG1	AX-85199780	69.34
LG1	AX-85233091	69.34
LG1	AX-85288827	69.34
LG1	AX-85309897	69.34
LG1	AX-85262782	69.37
LG1	AX-85424078	69.37
LG1	AX-85342895	69.45
LG1	AX-85394353	69.55

LG1	AX-85420545	69.55
LG1	AX-85201298	69.72
LG1	AX-85214455	69.72
LG1	AX-85230934	69.72
LG1	AX-85322787	69.72
LG1	AX-85354075	69.72
LG1	AX-85355753	69.72
LG1	AX-85419525	69.72
LG1	AX-85434771	69.72
LG1	AX-86136662	69.72
LG1	AX-85405451	69.73
LG1	AX-85419900	69.73
LG1	AX-86102629	69.73
LG1	AX-85353451	69.78
LG1	AX-85195536	69.8
LG1	AX-85427685	69.84
LG1	AX-85396074	69.85
LG1	AX-85211564	70.02
LG1	AX-85223740	70.02
LG1	AX-85400450	70.02
LG1	AX-85205027	70.11
LG1	AX-85220051	70.11
LG1	AX-85244142	70.11
LG1	AX-85290398	70.11
LG1	AX-85357988	70.11
LG1	AX-86098123	70.11
LG1	AX-85231028	70.13
LG1	AX-85296193	70.13
LG1	AX-85309930	70.13
LG1	AX-85331616	70.13
LG1	AX-85381974	70.13
LG1	AX-85386316	70.13
LG1	AX-85411572	70.13
LG1	AX-85438592	70.13
LG1	AX-85212115	70.17
LG1	AX-85213519	70.18
LG1	AX-85264158	70.18
LG1	AX-85377321	70.18
LG1	AX-86137095	70.2
LG1	AX-85330790	70.21
LG1	AX-85202932	70.25
LG1	AX-85311943	70.25
LG1	AX-85435636	70.25
LG1	AX-86116552	70.25
LG1	AX-85363632	70.28
LG1	AX-85247075	70.44
LG1	AX-85298363	70.44
LG1	AX-85229806	70.5
LG1	AX-85381708	70.5
LG1	AX-85434369	70.5

LG1	AX-85999663	70.7
LG1	AX-85193194	70.75
LG1	AX-85342854	70.75
LG1	AX-86118543	70.75
LG1	AX-85328375	71.1
LG1	AX-85207886	71.34
LG1	AX-85201573	71.36
LG1	AX-85378185	71.36
LG1	AX-86036251	71.51
LG1	AX-85192227	71.59
LG1	AX-85330339	71.59
LG1	AX-85275083	71.64
LG1	AX-85302523	71.64
LG1	AX-85352600	71.64
LG1	AX-85197504	72.52
LG1	AX-85387253	72.52
LG1	AX-85225258	72.8
LG1	AX-85335342	72.8
LG1	AX-85360172	72.8
LG1	AX-85392752	72.8
LG1	AX-86052004	72.8
LG1	AX-85217262	73.05
LG1	AX-85341203	73.05
LG1	AX-85355344	73.28
LG1	AX-85241897	73.47
LG1	AX-85247912	73.47
LG1	AX-85324512	73.47
LG1	AX-85353376	73.47
LG1	AX-85370737	73.47
LG1	AX-85433956	73.47
LG1	AX-86087391	73.47
LG1	AX-85411758	73.55
LG1	AX-85209676	73.62
LG1	AX-86155307	73.66
LG1	AX-85256029	73.7
LG1	AX-85397920	73.7
LG1	AX-86113492	73.7
LG1	AX-85394045	73.91
LG1	AX-85314114	74.22
LG1	AX-85312494	74.36
LG1	AX-85418537	74.47
LG1	AX-85284457	74.5
LG1	AX-85313556	74.5
LG1	AX-85392537	74.5
LG1	AX-85395086	74.5
LG1	AX-85334971	74.83
LG1	AX-85345241	74.83
LG1	AX-85202380	74.88
LG1	AX-85229110	74.88
LG1	AX-85351218	74.88

LG1	AX-86088519	75.36
LG1	AX-85232723	75.41
LG1	AX-85262167	75.41
LG1	AX-85345036	75.41
LG1	AX-85227928	75.5
LG1	AX-85238141	75.5
LG1	AX-85246973	75.5
LG1	AX-85318020	75.5
LG1	AX-85340960	75.5
LG1	AX-85350818	75.5
LG1	AX-85381766	75.5
LG1	AX-85438461	75.5
LG1	AX-86050025	75.54
LG1	AX-85341667	75.65
LG1	AX-85219844	75.7
LG1	AX-85252279	75.7
LG1	AX-85254206	75.7
LG1	AX-85301033	75.7
LG1	AX-85317586	75.7
LG1	AX-85317966	75.7
LG1	AX-85372306	75.7
LG1	AX-85424088	75.7
LG1	AX-85229264	75.77
LG1	AX-86065358	75.77
LG1	AX-85441109	76.14
LG1	AX-85225611	76.19
LG1	AX-85270626	76.19
LG1	AX-86053556	76.19
LG1	AX-85238859	76.46
LG1	AX-85405684	76.46
LG1	AX-85406754	76.46
LG1	AX-85423769	76.46
LG1	AX-85424944	76.46
LG1	AX-85243439	76.48
LG1	AX-85412864	76.66
LG1	AX-85370445	76.69
LG1	AX-85431184	76.73
LG1	AX-85409511	76.8
LG1	AX-85289683	76.89
LG1	AX-85404500	76.93
LG1	AX-85285382	77.18
LG1	AX-85437345	77.18
LG1	AX-85195102	77.3
LG1	AX-85284146	77.36
LG1	AX-85364478	77.36
LG1	AX-85374282	77.36
LG1	AX-85314411	77.42
LG1	AX-85324364	77.42
LG1	AX-85376225	77.42
LG1	AX-85393412	77.42

LG1	AX-85236745	77.49
LG1	AX-85247620	77.49
LG1	AX-85307663	77.49
LG1	AX-85332951	77.49
LG1	AX-86155833	77.49
LG1	AX-85321238	77.69
LG1	AX-85275288	77.71
LG1	AX-85390254	77.71
LG1	AX-85423711	77.8
LG1	AX-85280014	77.82
LG1	AX-85283568	77.82
LG1	AX-85376336	78.33
LG1	AX-85288862	78.5
LG1	AX-85201374	78.53
LG1	AX-85274566	78.65
LG1	AX-86048354	78.87
LG1	AX-85236041	79.13
LG1	AX-85270472	79.34
LG1	AX-85417512	79.52
LG1	AX-86100039	79.8
LG1	AX-85205421	79.85
LG1	AX-85341549	79.85
LG1	AX-85395117	79.9
LG1	AX-85218726	79.93
LG1	AX-85310508	79.93
LG1	AX-85289068	80.24
LG1	AX-85947183	80.24
LG1	AX-85213991	80.43
LG1	AX-85308260	80.55
LG1	AX-85198504	80.8
LG1	AX-85307948	80.8
LG1	AX-85378769	80.8
LG1	AX-85956591	80.8
LG1	AX-85211728	80.84
LG1	AX-85347085	81.12
LG1	AX-85198066	81.27
LG1	AX-85230798	81.27
LG1	AX-85265588	81.27
LG1	AX-85311067	81.27
LG1	AX-85332033	81.27
LG1	AX-85368207	81.27
LG1	AX-85202839	81.55
LG1	AX-85365630	81.55
LG1	AX-85932229	81.55
LG1	AX-85428876	81.57
LG1	AX-85948524	81.61
LG1	AX-85288909	81.76
LG1	AX-86028439	81.78
LG1	AX-85331896	82.06
LG1	AX-85335747	82.06

LG1	AX-85409447	82.06
LG1	AX-85969698	82.23
LG1	AX-85331337	82.38
LG1	AX-85355520	82.38
LG1	AX-85303556	82.48
LG1	AX-85390203	82.48
LG1	AX-85266238	82.73
LG1	AX-85308853	82.89
LG1	AX-85303819	82.94
LG1	AX-85270948	83.24
LG1	AX-85392284	83.24
LG1	AX-85297905	83.4
LG1	AX-85344409	83.55
LG1	AX-85231529	83.85
LG1	AX-85296642	83.85
LG1	AX-85325325	83.85
LG1	AX-85339437	83.85
LG1	AX-85385480	83.85
LG1	AX-85199081	83.88
LG1	AX-85215714	84.05
LG1	AX-85234868	84.19
LG1	AX-85235335	84.19
LG1	AX-85351527	84.46
LG1	AX-85361581	84.46
LG1	AX-85423659	84.46
LG1	AX-85929984	84.46
LG1	AX-85216019	84.91
LG1	AX-85267047	84.91
LG1	AX-85950632	84.91
LG1	AX-85382639	84.93
LG1	AX-85411638	85.26
LG1	AX-85296502	85.53
LG1	AX-85357079	85.53
LG1	AX-86081198	85.85
LG1	AX-85233154	85.86
LG1	AX-85438903	85.87
LG1	AX-85406733	86.15
LG1	AX-85354203	86.35
LG1	AX-85332537	86.41
LG1	AX-85214016	87.11
LG1	AX-85217766	87.11
LG1	AX-85373526	87.11
LG1	AX-85394575	87.14
LG1	AX-85209873	87.18
LG1	AX-85368792	87.2
LG1	AX-85432690	87.2
LG1	AX-86054566	87.34
LG1	AX-85273552	87.67
LG1	AX-85317793	87.67
LG1	AX-86140304	87.67

LG1	AX-85232787	88.06
LG1	AX-85250884	88.32
LG1	AX-85273538	88.32
LG1	AX-85332161	88.38
LG1	AX-86106203	88.52
LG1	AX-85422840	89.39
LG1	AX-85311061	89.56
LG1	AX-86141418	89.56
LG1	AX-86051060	89.79
LG1	AX-85385350	90.13
LG1	AX-85425078	90.13
LG1	AX-85327528	90.79
LG1	AX-85369087	90.87
LG1	AX-85424808	90.87
LG1	AX-85197211	90.9
LG1	AX-85424323	90.9
LG1	AX-85263575	91.07
LG1	AX-85287397	91.07
LG1	AX-85222579	91.21
LG1	AX-85308829	91.47
LG1	AX-85365523	91.54
LG1	AX-85320008	91.8
LG1	AX-85362775	91.89
LG1	AX-85203875	92.11
LG1	AX-85253259	92.11
LG1	AX-85264815	92.11
LG1	AX-85271338	92.11
LG1	AX-85939613	92.11
LG1	AX-85376691	92.69
LG1	AX-85254201	92.98
LG1	AX-85399086	93.1
LG1	AX-85233325	93.33
LG1	AX-85247927	94.08
LG1	AX-85266643	94.11
LG1	AX-85351898	94.12
LG1	AX-85305721	94.6
LG1	AX-85932494	94.67
LG1	AX-85431985	94.68
LG1	AX-85243679	94.78
LG1	AX-85365611	94.9
LG1	AX-85240532	95.07
LG1	AX-85195062	95.96
LG1	AX-85233076	95.96
LG1	AX-85292497	95.96
LG1	AX-85294166	95.96
LG1	AX-85379801	95.96
LG1	AX-85969289	96.05
LG1	AX-85213178	96.08
LG1	AX-85434670	96.32
LG1	AX-85202185	96.7

LG1	AX-85433033	96.7
LG1	AX-85251503	96.95
LG1	AX-85409892	97.26
LG1	AX-85250802	97.53
LG1	AX-85290561	97.53
LG1	AX-85274077	98.04
LG1	AX-85366553	98.26
LG1	AX-85391568	98.54
LG1	AX-86056708	98.57
LG1	AX-85203629	98.68
LG1	AX-85386719	98.76
LG1	AX-85212318	99.14
LG1	AX-85362431	99.25
LG1	AX-85197481	99.32
LG1	AX-85211030	99.49
LG1	AX-85275031	99.49
LG1	AX-85296708	99.49
LG1	AX-85366073	99.59
LG1	AX-85228398	99.8
LG1	AX-85191338	99.9
LG1	AX-85311116	99.9
LG1	AX-85242737	99.98
LG1	AX-85373832	100.11
LG1	AX-86012049	100.4
LG1	AX-86135392	100.79
LG1	AX-85201181	101.54
LG1	AX-85189634	101.58
LG1	AX-85254306	101.8
LG1	AX-85391464	101.8
LG1	AX-85218783	102.24
LG1	AX-85287122	102.64
LG1	AX-85193277	102.81
LG1	AX-85292139	103.16
LG1	AX-85313839	103.16
LG1	AX-85244533	103.75
LG1	AX-85380328	103.75
LG1	AX-85205822	104.63
LG1	AX-85440919	104.63
LG1	AX-85200571	105.11
LG1	AX-85420879	105.11
LG1	AX-85360261	105.28
LG1	AX-85245707	105.65
LG1	AX-85224085	106.26
LG1	AX-86057229	106.76
LG1	AX-85221093	106.8
LG1	AX-85408930	107.21
LG1	AX-85255944	107.39
LG1	AX-85299213	107.39
LG1	AX-85251550	107.67
LG1	AX-85259273	107.67

LG1	AX-85332976	107.67
LG1	AX-85959399	107.75
LG1	AX-85940793	108.53
LG1	AX-85306887	108.99
LG1	AX-85438996	109.17
LG1	AX-85243838	109.33
LG1	AX-86003422	109.73
LG1	AX-85270961	109.8
LG1	AX-85276676	109.8
LG1	AX-85346862	109.8
LG1	AX-85193103	110.09
LG1	AX-85237857	110.43
LG1	AX-85223571	111.81
LG1	AX-85368827	111.81
LG1	AX-85952573	111.81
LG1	AX-85252263	112.02
LG1	AX-85215037	112.27
LG1	AX-85222108	112.27
LG1	AX-85250304	112.27
LG1	AX-85333147	112.27
LG1	AX-85290243	112.58
LG1	AX-85406780	112.63
LG1	AX-85300519	112.8
LG1	AX-85313466	113
LG1	AX-86071543	113.11
LG1	AX-86039697	114.24
LG1	AX-85226023	114.7
LG1	AX-85372486	115.03
LG1	AX-85226001	115.85
LG1	AX-85296142	115.85
LG1	AX-85202565	115.87
LG1	AX-85273822	115.87
LG1	AX-85304443	115.87
LG1	AX-85323703	115.87
LG1	AX-85330967	115.87
LG1	AX-85260203	115.9
LG1	AX-85280439	116.2
LG1	AX-85311301	116.2
LG1	AX-85389205	116.2
LG1	AX-85193568	116.63
LG1	AX-85314961	116.63
LG1	AX-85340421	116.63
LG1	AX-85326826	116.65
LG1	AX-85926177	117.09
LG1	AX-85344880	117.28
LG1	AX-85317661	117.51
LG1	AX-85386881	117.51
LG1	AX-85390628	117.52
LG1	AX-85302125	117.81
LG1	AX-85314869	117.81

LG1	AX-85339816	117.9
LG1	AX-85328251	118.06
LG1	AX-85373370	118.84
LG1	AX-85328694	119.36
LG1	AX-85283591	119.6
LG1	AX-86110275	119.71
LG1	AX-85268019	119.74
LG1	AX-85259207	120.02
LG1	AX-85273784	120.02
LG1	AX-85349753	120.02
LG1	AX-86138537	120.31
LG1	AX-85229179	121.32
LG1	AX-85301172	121.32
LG1	AX-85435975	121.48
LG1	AX-85324499	121.95
LG1	AX-85379719	121.95
LG1	AX-85425422	122.02
LG1	AX-86073375	122.32
LG1	AX-85289922	122.53
LG1	AX-85255070	122.69
LG1	AX-85364181	122.69
LG1	AX-85294564	123
LG1	AX-85283331	123.58
LG1	AX-85350882	124.22
LG1	AX-85198085	124.44
LG1	AX-85374041	124.44
LG1	AX-85920648	124.73
LG1	AX-85258513	124.88
LG1	AX-86033645	124.88
LG1	AX-85363040	125.23
LG1	AX-85395226	125.34
LG1	AX-86109229	126.08
LG1	AX-85273617	126.17
LG1	AX-85298127	126.28
LG1	AX-85314348	126.28
LG1	AX-85407657	127.17
LG1	AX-85193565	127.24
LG1	AX-86107059	127.28
LG1	AX-85314128	127.55
LG1	AX-85329256	127.89
LG1	AX-85189441	127.91
LG1	AX-85237779	127.91
LG1	AX-85282284	127.91
LG1	AX-85245022	128.25
LG1	AX-85270125	128.58
LG1	AX-85283090	128.58
LG1	AX-85292394	128.58
LG1	AX-85333357	128.58
LG1	AX-85409691	128.58
LG1	AX-85954229	128.58

LG1	AX-85312202	129.28
LG1	AX-85355755	129.55
LG1	AX-85241765	129.74
LG1	AX-85322535	129.74
LG1	AX-85365476	129.74
LG1	AX-85405282	129.74
LG1	AX-85935037	129.74
LG1	AX-85338683	130.1
LG1	AX-85213560	130.39
LG1	AX-85331559	130.39
LG1	AX-85351761	130.39
LG1	AX-85353754	130.9
LG1	AX-85393656	130.9
LG1	AX-85269923	130.99
LG1	AX-85280931	130.99
LG1	AX-85227567	131.08
LG1	AX-85215991	131.44
LG1	AX-85191566	131.57
LG1	AX-85267203	131.57
LG1	AX-85368689	131.57
LG1	AX-86130463	131.76
LG1	AX-85206637	132.02
LG1	AX-85377883	132.02
LG1	AX-85306876	133.29
LG1	AX-85198876	133.53
LG1	AX-85353254	133.53
LG1	AX-85323831	134.18
LG1	AX-85339908	134.62
LG1	AX-85349280	134.7
LG1	AX-85438561	134.7
LG1	AX-85392357	134.91
LG1	AX-85366717	135.23
LG1	AX-85415340	135.58
LG1	AX-85304875	135.86
LG1	AX-85375762	135.93
LG1	AX-85217954	135.98
LG1	AX-85358836	136.21
LG1	AX-85325043	136.61
LG1	AX-85202999	137.02
LG1	AX-85255701	137.14
LG1	AX-85370144	137.14
LG1	AX-85206874	137.27
LG1	AX-85251404	137.27
LG1	AX-85297090	137.27
LG1	AX-85323565	137.27
LG1	AX-85364060	137.27
LG1	AX-85376484	137.27
LG1	AX-85382447	137.27
LG1	AX-85390001	137.27
LG1	AX-85393763	137.27

LG1	AX-85414506	137.27
LG1	AX-86016579	137.27
LG1	AX-85201257	137.34
LG1	AX-85309277	137.34
LG1	AX-85357505	137.34
LG1	AX-85269623	137.45
LG1	AX-86144850	137.45
LG1	AX-85190918	137.52
LG1	AX-85198183	137.52
LG1	AX-85198718	137.52
LG1	AX-85336672	137.52
LG1	AX-85355707	137.52
LG1	AX-85342155	137.63
LG1	AX-85343286	137.63
LG1	AX-85359275	137.9
LG1	AX-85429308	137.98
LG1	AX-85297363	138
LG1	AX-85281980	138.09
LG1	AX-85289440	138.22
LG1	AX-85190049	138.27
LG1	AX-85192094	138.27
LG1	AX-85207902	138.27
LG1	AX-85224767	138.27
LG1	AX-85232061	138.27
LG1	AX-85246285	138.27
LG1	AX-85267275	138.27
LG1	AX-85276030	138.27
LG1	AX-85311849	138.27
LG1	AX-85316814	138.27
LG1	AX-85334400	138.27
LG1	AX-85395470	138.27
LG1	AX-85240468	138.35
LG1	AX-85422817	138.36
LG1	AX-85322999	138.42
LG1	AX-85259016	138.46
LG1	AX-85204038	138.59
LG1	AX-85217190	138.7
LG1	AX-86158059	138.71
LG1	AX-85283571	138.84
LG1	AX-85399503	138.94
LG1	AX-85241158	139.13
LG1	AX-86043016	139.48